Cerebral Cortex September 2009;19:2038–2064
doi:10.1093/cercor/bhn229
Advance Access publication February 16, 2009

Thalamocortical Connections of Parietal Somatosensory Cortical Fields in Macaque Monkeys are Highly Divergent and Convergent

Jeffrey Padberg[1], Christina Cerkevich[2], James Engle[1,3], Alexander T. Rajan[1], Gregg Recanzone[1,4], Jon Kaas[2] and Leah Krubitzer[1,3]

[1]Center for Neuroscience, University of California, Davis, Davis, CA, USA, [2]Department of Psychology, Vanderbilt University, Nashville, TN 37201, USA, [3]Department of Psychology and [4]Department of Neurobiology, Physiology & Behavior, University of California, Davis, Davis, CA 95618, USA

We examined the organization and cortical projections of the somatosensory thalamus using multiunit microelectrode recording techniques in anesthetized monkeys combined with neuroanatomical tracings techniques and architectonic analysis. Different portions of the hand representation in area 3b were injected with different anatomical tracers in the same animal, or matched body part representations in parietal areas 3a, 3b, 1, 2, and areas 2 and 5 were injected with different anatomical tracers in the same animal to directly compare their thalamocortical connections. We found that the somatosensory thalamus is composed of several representations of cutaneous and deep receptors of the contralateral body. These nuclei include the ventral posterior nucleus, the ventral posterior superior nucleus, the ventral posterior inferior nucleus, and the ventral lateral nucleus. Each nucleus projects to several different cortical fields, and each cortical field receives projections from multiple thalamic nuclei. In contrast to other sensory systems, each of these somatosensory cortical fields is uniquely innervated by multiple thalamic nuclei. These data indicate that multiple inputs are processed simultaneously within and across several, "hierarchically connected" cortical fields.

Keywords: area 1, area 2, area 5, posterior parietal cortex, topographic connections

Introduction

Somatosensory cortical areas 3a, 3b, 1, and 2 of anthropoid primates contain systematic representations of the receptors of the contralateral half of the body, and neurons in these areas are driven by one or more subclasses of receptors such as slowly or rapidly adapting cutaneous receptors, muscle spindles, and Golgi tendon organs (see Krubitzer and Disbrow 2008, for review). These representations parallel each other in somatotopic organization so that the hindlimb, trunk, forelimb and face are represented in a mediolateral sequence in each of these areas. This pattern of parallel representation continues into the rostral portion of the posterior parietal cortex in regions generally designated as areas 5 and 7b in macaque monkeys. In these 2 areas, representations of the forelimb and face parallel those in the subdivisions of anterior parietal fields of cortex (Fig. 1). Although studies in awake monkeys provide important information on the stimulus conditions under which neurons in each of these areas are active, fundamental questions regarding how information is processed in the somatosensory system still remain. For example, is the somatosensory system like the visual system in which a clear segregation of inputs is present at both the level of the thalamus and the level of the cortex, and is information processed in a similar hierarchical fashion? How is information from different receptors combined within and across these fields to extract sensory information necessary for texture and shape discrimination, object identification and recognition, and more complex abilities such as generating body or limb centered coordinates necessary for intentional reaching and grasping (Randolph and Semmes 1974; Carlson 1981; Schwartz 1983; Gardner 1988; Ferraina and Bianchi 1994; Lacquaniti et al. 1995; Snyder et al. 1997; Debowy et al. 2001; see Krubitzer and Disbrow 2008, for review)?

Previous studies of the connections of these individual areas have lead to several important observations that contribute to our understanding of thalamocortical processing networks and begin to address the questions posed above. First, each of the 4 fields in anterior parietal cortex receives input from several different thalamic nuclei including the ventral posterior nucleus (VP), the ventral posterior inferior nucleus (VPi), a recently distinguished subdivision of the ventral posterior complex (Table 1), the ventral posterior superior nucleus (VPs), the anterior pulvinar (Pla), and one of the nuclei of the motor thalamus, the posterior division of the ventral lateral nucleus (VLp; see Jones 2007; Kaas 2008, for review; see Discussion for alternate nomenclature). Second, these nuclei project with different magnitudes to these cortical areas, providing mixtures of information from several nuclei to each cortical field. Third, as most or all of these nuclei also contain systematic representations of the contralateral body (Mountcastle and Henneman 1952; Poggio and Mountcastle 1963; Jones and Friedman 1982; Kaas et al. 1984; Rausell and Jones 1991), thalamocortical projections are at least roughly somatotopic (Rausell et al. 1998), and for some areas, provide activating input that generates the cortical representation.

The existence of both cortical and thalamic somatotopic representations suggest that the same group of neurons that project to a given part of one cortical representation also projects to somatotopically matched parts of other representations that are targets of that nucleus. Possibly some or many of these neurons in such a cell group would project to more than one cortical area. Alternatively, thalamic nuclei could consist of modules of cells distinguished by projections to different cortical areas, as well as other characteristics. Thus, adjoining clusters of neurons would project to different areas. Finally, thalamic projections to cortical areas may not be strictly somatotopic, so that the somatotopy that is revealed in cortical areas does not fully reflect the distribution of thalamic inputs, but rather is constrained by inhibitory circuits in cortex, or other mechanisms. Such exuberant projections could mediate some of the somatotopic reorganization of somatosensory cortex that follows partial sensory loss (e.g., Merzenich, Kaas,

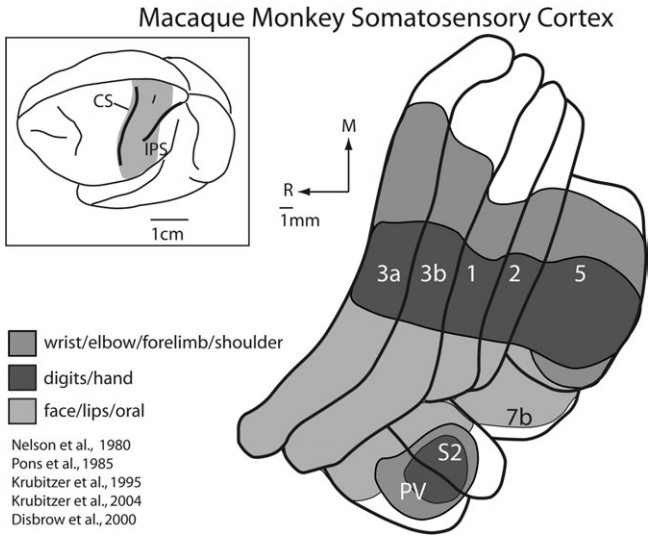

Figure 1. Somatosensory cortical areas in macaque monkeys. The shaded region in the top left illustration of the entire brain indicates the location of somatosensory cortical areas in macaque monkeys shown in the illustration to the right. These include area 3b, which is buried in the caudal bank of the central sulcus and area 3a, which is on the fundus and rostral bank of the central sulcus, although the position of area 3a can vary in different monkeys. Other somatosensory areas in anterior parietal cortex include areas 1 and 2, which reside on the postcentral gyrus. Area 5 is a posterior parietal field located on the rostral bank of the IPS, and areas S2 and the parietal ventral area (PV) are located on the upper bank of the lateral sulcus. Area 7b is also associated with somatosensory processing. The extent of the neocortex occupied by different body part representations within each of the cortical fields is indicated in a different color. Portions of the cortex devoted to the representations of the forelimb are shown in medium grey, portions of the cortex devoted to the representation of the hand and digits are indicated in dark grey, and portions of the cortex devoted to the representation of the face, lips and oral structures are indicated in light grey. There are 2 important features of organization of somatosensory areas. The first is that the representation of the face, hand and forelimb dominates all these fields. Second, at higher processing stages such as posterior parietal area 5, the cortical magnification of the hand and forelimb is further exaggerated, with only a small portion of the field devoted to other body part representations. See Table 1 for abbreviations.

Table 1
List of abbreviations

Cortical areas and sulci	
3a	Proprioceptive area in anterior parietal cortex
3b	Primary somatosensory area (S1)
1	Cutaneous somatosensory area in parietal cortex
2	Proprioceptive area in anterior parietal cortex
5	Somatosensory area in posterior parietal area
7b	Somatosensory area on the inferior parietal lobule
CS	Central sulcus
IPS	Intraparietal sulcus
S2	Second somatosensory area
PV	Parietal ventral area
Thalamic nuclei and midbrain structures	
AD	Anterodorsal nucleus
AV	Anteroventral nucleus
BSC	Brachium of the superior colliculus
CEM	Central medial nucleus
CL	Central lateral nucleus
CM	Centre médian nucleus
F	Fornix
HB	Habenular nucleus
LD	Lateral dorsal nucleus
LGd	Dorsal division of the lateral geniculate nucleus
LP	Lateral posterior nucleus
MD	Mediodorsal nucleus
MG	Medial geniculate nucleus
PAG	Periaquaductal grey matter
Pla	Anterior pulvinar nucleus
Pll	Lateral pulvinar nucleus
Plm	Medial pulvinar nucleus
VA	Ventral anterior nucleus
VLp	Posterior division of the ventral lateral nucleus
VMb	Basal ventral medial nucleus
VP	Ventral posterior nucleus
VPi	Ventral posterior inferior nucleus
VPl	Ventral posterior lateral nucleus
VPm	Ventral posterior medial nucleus
VPs	Ventral posterior superior nucleus
VP proper	VPl + VPm
VP complex	VPl, VPm, VPs, VPi
ZI	Zona incerta
Body parts	
cn	Chin
d1	Digit 1
d2	Digit 2
d3	Digit 3
d4	Digit 4
d5	Digit 5
fl	Forelimb
hl	Hindlimb
prox	Proximal
sh	Shoulder
t1	Toe 1
t2	Toe 2
t5	Toe 5
tr	Trunk
wr	Wrist
ul	Upper lip
Anatomical directions	
D	Dorsal
L	Lateral
M	Medial
R	Rostral
Anatomical tracers and histological stains	
Cat-301	Monoclonal antibody Cat-301
CB	Calbindin
CO	Cytochrome oxidase
BDA	Biotinylated dextran amine
DY	Diamidino yellow
FB	Fast blue
FE	Fluoroemerald
FG	Fluorogold
FR	Fluororuby
GB	Green fluorescent beads
NY	Nuclear yellow

Wall, Nelson, et al. 1983; Merzenich, Kaas, Wall, Sur, et al. 1983; Merzenich et al. 1984; see Kaas 2000).

Although a previous studies have examined the divergence and convergence of thalamocortical connectivity of different areas (e.g., Jones 1983), in this study only 2 fields were examined in any given animal, and injection sites were not topographically matched. We sought to address these issues by injecting a different anatomical tracer in 2 to 4 different cortical fields in the same monkey. Because the somatotopic location for each injection site was electrophysiologically determined, it was possible to inject tracers into the representation of the same body part in each cortical field. The size of receptive fields varies for neurons in different cortical areas so that in some cases the same size injection involved the representation of more body parts in some areas than in others. Despite this, injections could be placed in locations across areas where neurons had overlapping receptive fields. This set of experiments allowed us to directly compare the thalamocortical connections of matching representations across 5 different cortical areas and to test the hypothesis that there is a high degree of divergent and convergent connections from nuclei in the thalamus to each cortical field that results in a unique combination of inputs from different nuclei to the same body part representation in the different cortical fields. We addressed the issue of divergence of projections to a single field by placing several injections of different tracers within the representations of

adjacent or nearby body parts (e.g., digits and palm) to see how close projection patterns conformed to that predicted by somatotopic matching. If somatotopic matching is precise, then each representation would receive nonoverlapping projections from a distinct body part representation in the thalamus. If somatotopic matching is less precise, then each representation (e.g., digits and palm) within a cortical field would receive overlapping projections from the same and related body part representations in the thalamus, and possibly the same neuron within in the thalamus could project to 2 separate representations in the cortex. This experimental design also allowed us to test the hypothesis that there are convergent inputs to a single representation within area 3b from different body part representations in VPl and from different nuclei of the thalamus. Together, the results from these experiments provide a new understanding of the complexity of the thalamocortical projection patterns to multiple areas of the cortex.

Methods

Thalamocortical connections of areas 3a, 3b, 1, 2, and 5 were examined in 8 macaque monkeys (7 *Macaca mulatta* and 1 *Macaca radiata*) using neuroanatomical tracing techniques combined with electrophysiological recording techniques, and an architectonic identification of thalamic nuclei and cortical fields (Table 2). In these animals, neuroanatomical tracers were injected into electrophysiologically and architectonically defined representations of the hand and/or digits within each field. Labeled cells resulting from these injections were identified in the dorsal thalamus and related to architectonic boundaries, and in one case to electrophysiologically identified boundaries. Microelectrode recordings from one additional monkey were used to examine the functional organization of the ventral posterior complex (VPl, VPm, VPi, VPs) and its relationship to architectonic boundaries. All experimental protocols were approved by the Institution Animal Care and Use Committee of the University of California, Davis and Vanderbilt University Animal Care and Use Committee and conformed to the National Institutes of Health guidelines.

Injections of Anatomical Tracers

A total of 24 injections were made in different cortical areas in 8 animals (Table 2). For every case, animals were initially anesthetized with ketamine hydrochloride (10–35 mg/kg, im). The animals were then intubated and cannulated, and anesthesia was maintained with an inhaled anesthetic, isoflurane (1.5–3%). The animals were artificially ventilated and continuously infused with lactated Ringers solution (6 mL/kg/h, iv). The heart rate, respiration rate, temperature and expired CO_2 levels were monitored and maintained. Once an animal was anesthetized and stabilized, the skin was cut, the temporalis muscle was retracted and a craniotomy was performed over the anterior and posterior parietal cortex. The dura was cut and the dura flaps were carefully pulled away from the opening. A digital image was made of the exposed neocortex so that electrophysiological recording sites and injections could be directly related to the vasculature of the brain. Neuroanatomical tracers were injected into electrophysiologically defined portions of the hand and digit representations (see below). Injections of anatomical tracers were made with a calibrated Hamilton syringe that was lowered into the cortex with a stereotaxically guided micromanipulator. Injections of 0.2–0.4 μL of the fluorescent tracers fluoroemerald (FE, 7%; Invitrogen, Carlsbad, CA), fluororuby (FR, 7%; Invitrogen, Carlsbad, CA), fluorescent green beads (GB; Invitrogen, Carlsbad, CA) or biotinylated dextran amine (BDA, 10%; Invitrogen) were made into areas 3a, 3b, 1, 2, and 5, and fast blue (FB; Sigma-Aldrich, St Louis, MO), fluorogold (FG; Sigma-Aldrich), and diamidino yellow combined with nuclear yellow (DY/NY; Sigma-Aldrich), were placed into these areas as crystals (see Krubitzer et al. 1998, for details). In 2 cases, DY was diluted with 0.1 M phosphate buffer to make a 2% solution and 0.45–0.5μL were injected into area 2 (cases 7 and 8). Finally, in 2 cases, 0.6 μL of Cholera Toxin Subunit-B (CTB; 1% in distilled water) was injected into area 5 (cases 7 and 8). After the injections were complete, the brain was covered with a sterile contact lens, the dura flaps were folded over the contact lens, and the skull was replaced and held in place with acrylic, or a new skull was made from acrylic. After the acrylic hardened, the temporal muscle was sutured in place and the skin was sutured together. The animal then recovered and was closely monitored for 8–14 days until transport of the tracers was complete.

The injection site core and halo surrounding the injection site were included in our reconstructions of injection sites, and these boundaries were directly related to architectonic borders (see Krubitzer et al. 1998, for details on determining injection site spread). Injections ranged in size from 250 × 500 μm to 3 × 4 mm (largest for case no. 4, Fig. 10). The mean area for all injection sites, excluding the large area 2 injection in case no. 4, was 1.07 mm^2 (or 1.47 mm^2 including the area 2 injection in case no. 4). All but 2 injection sites (in the same case; no. 4) were restricted to the region of interest and the spread of injections into other areas is shown in Figure 10.

Electrophysiological Recording

Standard multiunit electrophysiological recording techniques were utilized to guide injection site locations in 7 animals. In one of these animals and in one additional animal, microelectrode recordings were made in the thalamus (Table 2). The anesthetic and surgical preparation for acute electrophysiological mapping experiments were similar to those described above.

For animals in which electrophysiological recordings were made to guide injection placement, the cortex was continually bathed in sterile saline. For acute electrophysiological experiments, silicone fluid was placed on the exposed cortex to protect the brain from desiccation. Electrophysiological recordings were made with low impedance tungsten microelectrodes (1–5 MΩ at 100 Hz; A-M Systems, Sequim, WA) and the neural response was amplified, filtered, monitored on an oscilloscope and a speaker. For recordings on the postcentral gyrus, the electrode was lowered into the cortex using a micromanipulator to a depth of 700–1000 μm. For recordings in the depths of the central and intraparietal sulci, the electrode was lowered into the cortex in increments of 250–500 μm with an hydraulic microdrive (Kopf

Table 2
Case information

Case no.	Area(s) injected	Tracer used	Representation injected	Plane of section	Section thickness (μm)
1	3b	FB	Middle glabrous d3	Coronal	50
	3b	DY	Thenar		
	3b	FR	Dorsal d3–d5		
2	No injections	—	—	Coronal	80
3	3a	FR	Distal glabrous d3–d4	Coronal	50
	3b	GB	Distal glabrous d3		
	1	FB	Distal glabrous d3		
	2	DY	Distal glabrous d3–d4		
4	3a	FB	Dorsal d2–d4	Coronal	50
	3b	GB	Glabrous d3		
	1	FR	Distal glabrous d3		
	2	FG	Glabrous d2–d4		
5	2	FR	Glabrous d2	Horizontal	80
	2	FE	Glabrous d1		
6	2	FE	Distal glabrous d1	Coronal	50
	5	FR	Glabrous d1		
	3b (not shown)	BDA	Distal d1		
	1 (not shown)	NY/DY	Distal d1		
7	2	DY	Proximal palm	Coronal	50
	5	CTB	Ventral wrist, radial hand, Dorsal d1		
8	2	DY	Tip of d1	Coronal	50
	5	CTB	Proximal hypothenar		
	1 (not shown)	FR			
9	2 (not shown)	NY/DY	Not mapped	Horizontal	80
	5 (not shown)	BDA	Not mapped		

Instruments, Tujunga, CA). In animals in which electrophysiological recordings were performed in the thalamus, we first identified the general location of thalamus using cortical sulcal landmarks. We have been able to consistently and efficiently identify the general location of the somatosensory thalamus below cortex located just rostromedial to the central sulcus. Once the location of the somatosensory thalamus was determined, recordings were made across a cortical grid (6 × 8 mm, 1 mm spacing), and recording began after the electrode was advanced 15 mm from the cortical surface. The electrode was then lowered with the microdrive in increments of 200–250 μm, and at each site, the contralateral body surface was stimulated, and receptive fields for neurons at that site were identified and drawn on diagrams of the monkey's body. Fine probes and brushes were used to stimulate cutaneous receptors, whereas light to moderate taps, limb manipulation, and pressure were used to stimulate deep receptors in joints and muscles. We characterized a receptive field as cutaneous if neurons responded to light touch on the skin or hair displacement, and we characterized a receptive field as "deep" if neurons required more forceful taps on the skin or squeezing or manipulation of the fingers or other parts of the body. Although some of the responses termed "deep" could reflect high threshold cutaneous afferents, and some responses termed "cutaneous" could represent proprioceptive afferents that are highly sensitive, we feel our use of traditional terminology (Mountcastle and Henneman 1952) reflects the general response characteristics of neurons in different thalamic nuclei. Visual stimulation consisted of full field flashes and light sweeps across the contralateral visual hemifield, and auditory stimulation consisted of clicks.

Selected recording sites were marked for later identification in histologically processed tissue in 1 of 2 ways. First, the recording electrode was dipped in a 7% solution of FB or DY/NY (in cases in which these tracers were not used to determine connections) and then inserted into the cortex and/or advanced into the thalamus. This served to mark the electrode angle (Fig. 2) and assist with the alignment of electrophysiological maps. Second, we placed electrolytic lesions (10 μA for 10 s) at strategic locations in the cortex and/or thalamus.

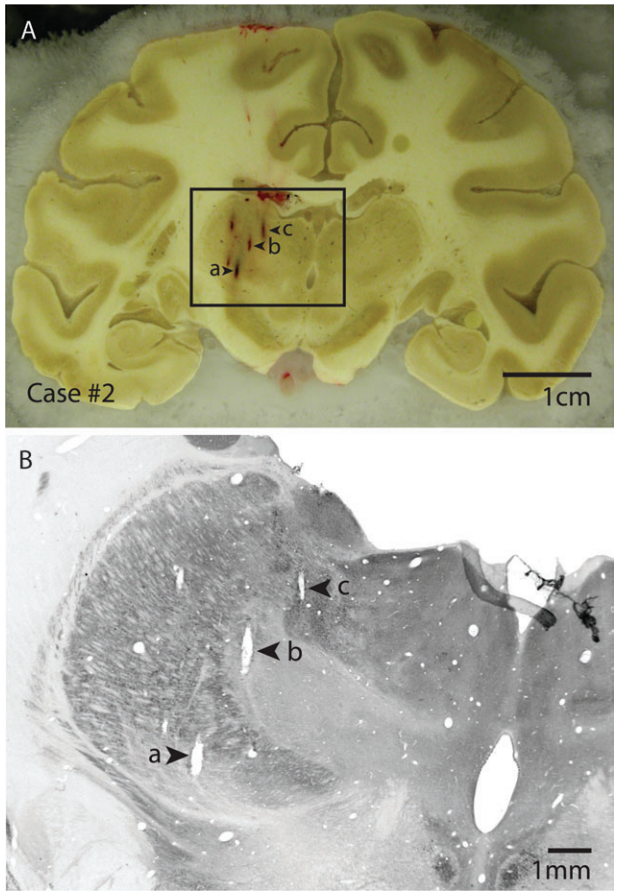

Figure 2. (*A*) Block-face image of a coronal section through the cortex and the thalamus in case #2 with electrode penetrations marked a, b, and c. The electrophysiological data reconstruction of this case is shown in detail in Figure 6, and electrode tracks a, b and c correspond to electrode tracks a, b and c between the 2 figures. (*B*) The section that corresponds to the block-face image in (*A*) has been processed for CO. Electrode penetrations a, b and c are readily identified in this section, and recording depths can be related to architectonic boundaries of thalamic nuclei. Block-face images combined with histologically processed sections that corresponded to each block-face image were used to guide the reconstruction of electrode penetrations from the dorsal portion of the thalamus through the ventral portion of the thalamus across sections. Dorsal is to the top and lateral is to the left.

Histological Processing

After the appropriate time had transpired for transport of tracer, or upon completion of the acute electrophysiological mapping portion of the experiment, each animal was euthanized with a lethal injection of sodium pentobarbital (60 mg/kg). The animal was then transcardially perfused with 0.9% saline, followed by 2–4% paraformaldehyde in phosphate buffer, and then 2–4% paraformaldehyde in 10% sucrose phosphate buffer (pH = 7.2–7.4). Following perfusion, the brain was carefully removed from the skull, and either remained intact or the hemispheres were removed from the thalamus. The brain was then placed in 30% sucrose phosphate buffer overnight prior to sectioning (Table 2).

In 7 cases the cortex was removed from the thalamus and flattened (Disbrow et al. 2003) and sectioned parallel to the surface on a freezing microtome. In these cases, the thalamus was sectioned coronally at a thickness of 50 μm. In the remaining cases the cortex and thalamus were sectioned horizontally at a thickness of 80 μm. Alternate series of sections were processed for Nissl, cytochrome oxidase (CO) histochemistry (CO: Wong-Riley, 1979), calbindin (CB; Celio 1990), Cat-301 (Hockfield et al. 1983), and/or myelin, mounted for fluorescence microscopy, and/or processed to reveal CTB (Bruce and Grofova 1992) or BDA (using standard avidin-biotin complex [ABC] methods). Sections processed for CO, CB, and Cat-301 usefully complemented the Nissl and myelin stains in revealing thalamic nuclei.

Data Analysis

Data analysis was performed in 3 separate stages and then all of the data were combined into comprehensive reconstructions. First, for both the cortex and the thalamus, the series of sections that were prepared for fluorescent microscopy or processed for BDA or CTB were analyzed using an x/y stage encoding system attached to a computer (Accustage, Inc., Shoreview, MN). For the entire series of sections in each case, labeled cells were identified in the thalamus and plotted along with tissue outlines, tissue artifacts and electrode tracks for alignment across the series. For the cortex, the injection site was plotted and included the central core as well as the surrounding halo. In our figures, the outer boundary of the injection site represents the outer boundary of the halo.

In the second stage of analysis, a camera lucida was used to align and draw boundaries from adjacent Nissl, CO, CB, Cat-301, and/or myelin stained sections. Once architectonic boundaries were drawn, cells in the thalamus resulting from each injection site were counted. For density determination, cells in a given nucleus resulting from an injection of one neuranatomical tracer was expressed as a percentage of the total number of labeled cells in the thalamus resulting from that injection. The data shown in Figure 7 represent the mean percentage of neurons for injections in a particular area in the different cases. For the cortex, electrophysiological recording data could be matched to individual sections by aligning the probes (fluorescent markers) and lesions made during the mapping phase of the experiments with the drawings of electrophysiological recording sites drawn on the photograph of the cortex. This allowed us to relate injection sites to electrophysiologically defined boundaries. These probes were identified in histologically processed tissue (see above) adjacent to the reconstructed fluorescent section that contained the injection site, and architectonic boundaries were drawn; this was done for the entire series of sections through the cortex (description of cortical

connections will be part of a subsequent study). By aligning probes, sulcal landmarks, injection site holes and other tissue artifacts injection sites could be related to both electrophysiological and architectonic boundaries. Criteria for determining boundaries between areas 4, 3a, 3b, 1, 2, and 5 have been well described in previous studies in our own laboratories and other laboratories (Pons et al. 1985; see Kaas 2008 for review), and these same criteria have been used in the present study as well (Fig. 3*A*,*B*)

For the final stage of our analysis, electrophysiological maps of the thalamus were drawn in relation to electrode depth and architectonic distinctions. Probes were identified in block-face images of the brain and related to architectonic boundaries and electrode tracks found in that same section (Fig. 2). Electrode tracks were identified and related to the microlesions and the probes inserted during our thalamic recording experiments. The electrode tracks often ran through several sections. For each section, architectonic boundaries were drawn, and in one of the cases plotted labeled cells were drawn by matching probe, lesion, tissue artifacts, blood vessels and tissue outlines. Comprehensive reconstructions were drawn using Adobe Illustrator (Adobe Systems, San Jose, CA) and digital images of labeled cells and histologically processed tissue were generated with a Spot RT Slider camera system (Diagnostic Instruments, Sterling Heights, MI). Minor adjustments of contrast and sharpness of digital images were performed with Adobe Photoshop (Adobe Systems).

Results

The thalamocortical connections of areas 3a, 3b, 1, 2, and 5 have been described in previous studies in macaque monkeys (Krubitzer and Disbrow 2008, for review). However, the present investigation differs in several important ways from most previous studies. First, for all but one case injections were placed into electrophysiologically identified representations of body parts of each cortical field and related to architectonically defined boundaries (Fig. 3*A*,*B*). Second, in cases in which connections of different cortical fields were examined, the same or overlapping body part representations were injected. All but one of these injections was restricted to the field of interest. Finally, for one case, connections of different electrophysiologically identified portions of the hand representation in area 3b were examined and related not only to architectonically defined nuclei of the thalamus, but to functionally defined representations of the thalamus as well (Fig. 3*C*–*F*). Although microelectrode recordings have been used to identify injection sites in somatosensory cortex (e.g., Pons and Kaas 1985b; Cusick et al. 1986) our combination of electrophysiological identification of somatotopically matched injection sites in multiple cortical areas in the same animal, together with the electrophysiological identification of thalamic nuclei projecting to these areas, has not been reported for any species of primate.

Functional and Architectonic Organization of the Somatosensory Thalamus

The ventral posterior nucleus and its medial (VPm) and lateral (VPl) subnuclei

In 2 monkeys (cases no. 1 and 2), the somatosensory thalamus was explored using electrophysiological recording techniques and these recordings were directly related to architectonic boundaries of the nuclei as defined using different histological stains (Figs 2 and 3). Three separate somatosensory nuclei could be readily defined by the tactile submodality that elicited neuronal responses, receptive field size of neurons, topographic organization, and architectonic appearance. The first nucleus was the ventral posterior nucleus, composed of a lateral and medial divisions, VPl and VPm, respectively. In both subnuclei, neurons responded to cutaneous stimulation of the contralateral body, face and oral structures, and had small receptive fields (Figs 4–6). In one case (no. 1) neurons at some recording sites in VP responded to higher threshold stimulation. As described in previous reports (e.g., Mountcastle and Henneman 1952; Poggio and Mountcastle 1963; Loe et al. 1977; Rausell and Jones 1991). VPl contained a complete representation of the contralateral body and was topographically organized. Within VPl, the upper trunk and shoulder were represented posteriorly in the mediodorsal portion of VPl and the lower trunk and hindlimb were represented more laterally at this level (Fig. 4). At more anterior levels, the tail was represented at the lateral edge of VPl and the foot, hand and wrist were represented in a successively more medial position. At this same level, the toes were represented ventral to the hindlimb and foot and the digits were represented ventral to the hand representation. Within the digit representation of the hand, proximal digits were represented dorsal to the distal digits, and D1 was represented medial to D2–D5 (Figs 4–6). As in previous studies (e.g., Mountcastle and Henneman 1952; Jones and Friedman 1982; Kaas et al. 1984; Rausell and Jones 1991; see Jones 2007; Kaas 2008, for review), the face, chin and oral structures were represented in VPm. Within VPm, the chin was represented in the dorsomedial portion of the posterior aspect of this subnucleus, and the tongue and oral structures were located medially and ventrally at more anterior portions of this subnucleus.

When electrophysiological recording data were related to histologically processed tissue, recording sites within the functionally defined VPl and VPm were within these subnuclei defined architectonically (Fig. 3). In Nissl stained sections, both VPl and VPm contained darkly staining, densely packed cells that were separated by cell-sparse, finger-like septa considered to be extensions of VPi (see Krubitzer and Kaas 1992). VPl and VPm were also distinct in tissue stained for CO and CB. In CO stained sections, VPl and VPm were darkly staining, and subdivisions within each nucleus were separated by CO light septa, which corresponded to the cell light regions identified in Nissl stained tissue. Immunostaining for CB revealed a dense neuropil staining in VPm, with few stained neurons evident. Light to moderate neuropil staining was observed in VPl with CB immunostaining . In sections stained for Cat-301, dense neuropil staining was observed in VPm, with a few densely stained cell bodies visible, and moderate to dense neuropil staining was observed in VPl, with several densely stained cell bodies throughout the nucleus (Fig. 3). This staining pattern generally was very similar to that described by Hendry et al. (1988; Fig. 16*C*,*D*).

The ventral posterior inferior and superior nuclei

The VPi and VPs nuclei could also be distinguished both functionally and architectonically (Figs 3–6). Although VPi has been previously distinguished by its architecture, connections and functional properties of neurons (e.g., Dykes et al. 1981; Rausell and Jones 1991; Krubitzer and Kaas 1992; Disbrow et al. 2002; see Kaas 2008 for review) the somatotopy of VPi has not been fully described. As in previous studies, neurons in VPi were less responsive to cutaneous stimuli than those in VP, and activation usually depended on more intense stimulation, such

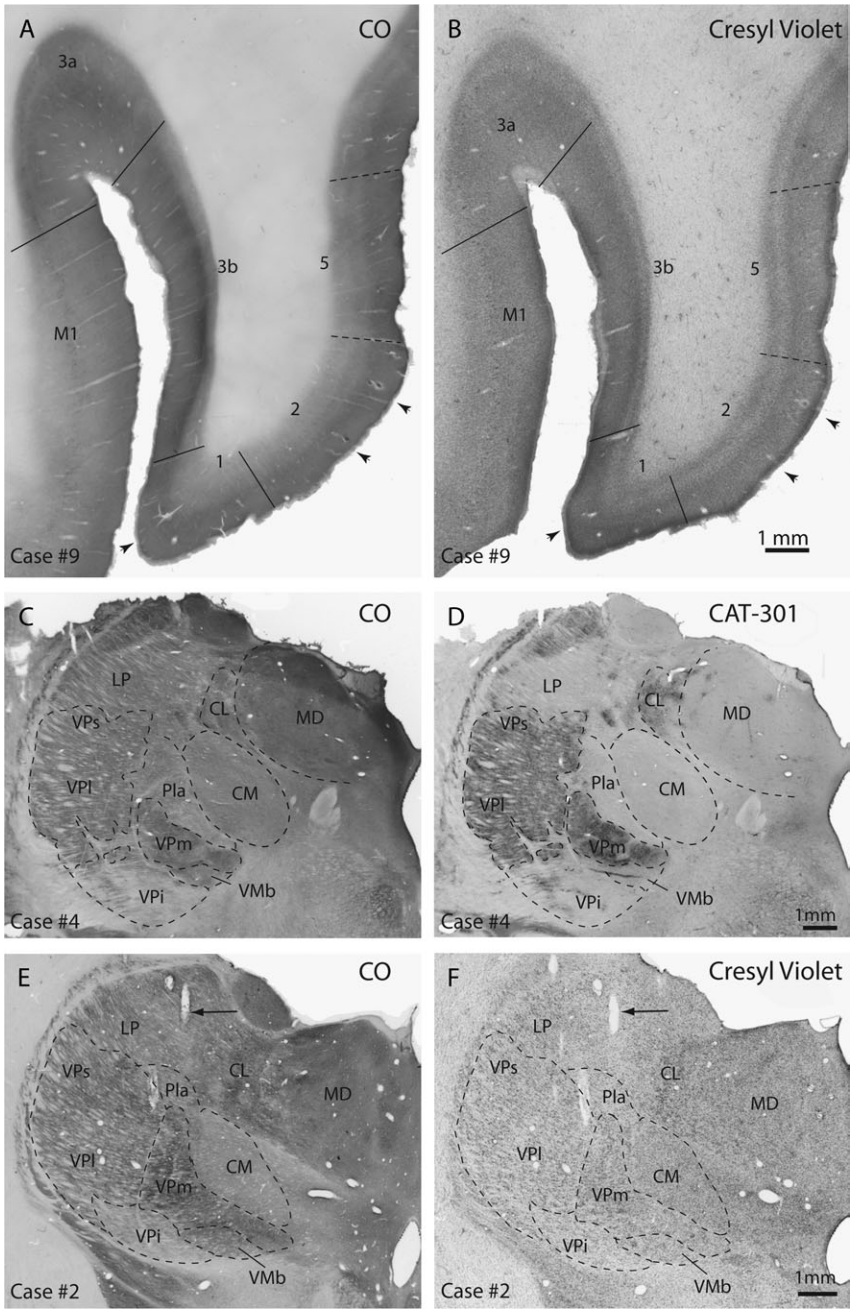

Figure 3. Horizontal sections from cortex from case no. 9 that has been reacted for CO (*A*) or stained with Cresyl violet (*B*). Cortical field boundaries are marked with solid lines and arrows point to electrode tracks in these adjacent sections. These architectonic boundaries were matched to electrophysiological recordings in the cortex in all cases to determine the borders of cortical areas and the location of injections sites within each area. Coronally sectioned portions of the dorsal thalamus from case no. 4 that have been stained for CO (*C*) and Cat-301 (*D*). Images E and F are from case no. 2 and have been stained for CO and Cresyl violet, respectively. In sections stained for CO, VP, and VPs stained darkly and VPi was lightly stained. The anterior pulvinar stained moderately for CO. In sections stained for Cat-301, LP stained lightly, making this nucleus readily distinguishable from VPl/VPs. Also, Pla stained lightly. In tissue stained for Nissl substance (*F*) VPm contained densely packed darkly stained cells and VPl and VPs contained densely packed cells that stained somewhat less darkly for Nissl. VPi contained loosely packed cells that stained lightly for Nissl. The arrows in E and F mark an electrode track through the tissue. Dashed lines mark architectonic boundaries of nuclei. The scale bar for all images is 1 mm. See Table 1 for abbreviations. Conventions as in previous figures.

as taps to the body. We did not test for responses to stimulation of Pacinian corpuscles in VPi, but such responses were observed in previous studies by Dykes et al. (1981). Receptive fields for neurons in VPi were large when compared with those for neurons in VPl or VPm (Fig. 6C). However, at some recording sites within VPi neurons responded to light cutaneous stimulation of the contralateral body (Fig. 4). The topographic organization of VPi roughly mirrors that of VPl and VPm. At posterior levels of the thalamus, the foot is represented in the dorsal lateral portion of the nucleus, and in case no. 1 is interdigitated between the foot and toes and digit representation of VPl. Ventral to the foot and hindlimb representation of VPi is the representation of the lower trunk and tail. Medial and rostral to the representation of the lower limb and toes is the

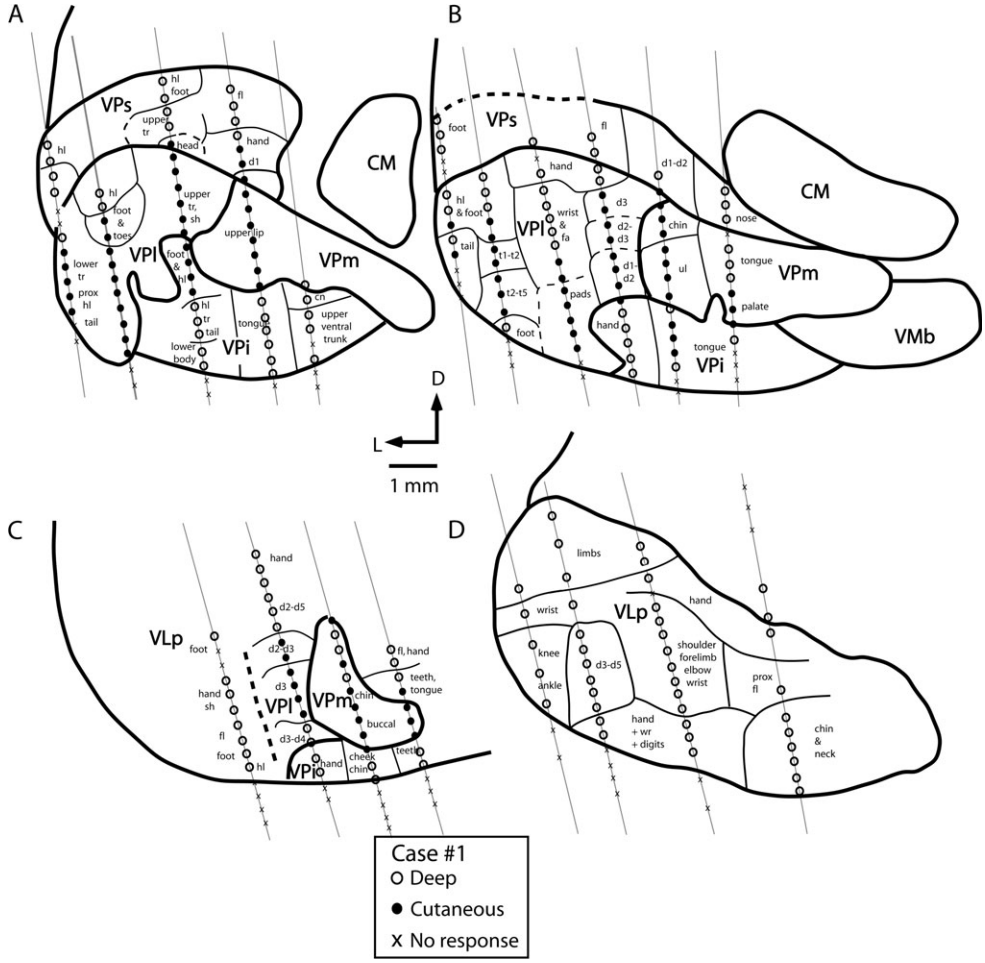

Figure 4. Coronal reconstructions of electrophysiological recordings from case no. 1. Electrode penetrations and architectonic boundaries have been collapsed across 3 sections for each illustrated section to better appreciate the topographic organization of the somatosensory nuclei of the thalamus. The distance between sections (*A*) and (*B*) is 150 μm, (*B*) and (*C*) is 350 μm, and (*C*) and (*D*) is 150 μm. Several nuclei could be readily distinguished using electrophysiological recording techniques. The ventral posterior nucleus contained neurons that responded to cutaneous stimulation of the contralateral body (VPl) and face (VPm; *A–C*). Just ventral to VP proper was a second representation of the contralateral body in which neurons responded to stimulation of deep receptors. This nucleus was coextensive with the architectonically defined VPi. The third nucleus is VPs (*A* and *B*). Neurons in VPs responded to stimulation of deep receptors of the contralateral body. There was a gross topographic organization of VPs that mirrored that of VPl and VPm. Finally, at the rostral boundary of VP proper, neurons responded to stimulation of deep receptors of the contralateral body; this representation was coextensive with the architectonically defined VLp (*D*). Thick lines denote architectonic boundaries of each nucleus and thin lines separate different body part representations within each nucleus. Dashed lines mark approximate architectonic boundaries. This series of sections and series on all remaining figures are drawn caudal (*A*) through rostral (*D*). See Table 1 for abbreviations. Conventions as in previous figures.

representation of portions of the forelimb including the pads laterally, and the hand and digits medial to this. In case no. 2, one electrode track was favorably located close to the small fingerlike projection of VPi that separates VPm from VPl (Fig. 6*B*, electrode track b). In this case, neurons that were recorded in that track responded to both cutaneous stimulation of the chin (from VPm) and more intense stimulation of the hand (from VPi fingerlike protrusion). Within VPi, the tongue is represented in a medial location, although at a few sites, responses to stimulation of the upper trunk were observed in a medial location (Fig. 4*A*). The chin is represented dorsal to the tongue. Anterior to this is the representation of the hand and digits laterally and the cheek and teeth more medially.

VPi is readily distinguished in a variety of different histological preparations. In Nissl stained sections VPi is very light in appearance and contains small loosely packed cells that form fingerlike protrusions into VPl and VPm. In CO and CB stained sections, VPi was very light in appearance. Cat-301 staining revealed a few densely labeled cell bodies within VPi, with patchy light to moderate staining of the neuropil, located near the cell bodies. (Fig. 3*C–E*).

VPs could also be distinguished functionally and architectonically although the architectonic border between VP and VPs was less well defined than the other borders of VPs. In early reports VPs was not distinguished from VP, although neurons in a dorsal capping zone (considered part of VP) were found to be responsive to stimulation of deep body receptors (e.g., Poggio and Mountcastle 1963; Loe et al. 1977). In the present study, neurons in VPs responded to stimulation of deep receptors of the contralateral body, and according to previous reports, these responses are largely mediated by muscle spindle receptors (see Wiesendanger and Miles 1982; Macchi and Jones 1997; Kaas 2008, for review). Further, there was a gross topographic organization of VPs that mirrored that of VP, but was not as precise (Figs 4–6). In posterior and mid thalamic sections, the hindlimb and foot were represented laterally,

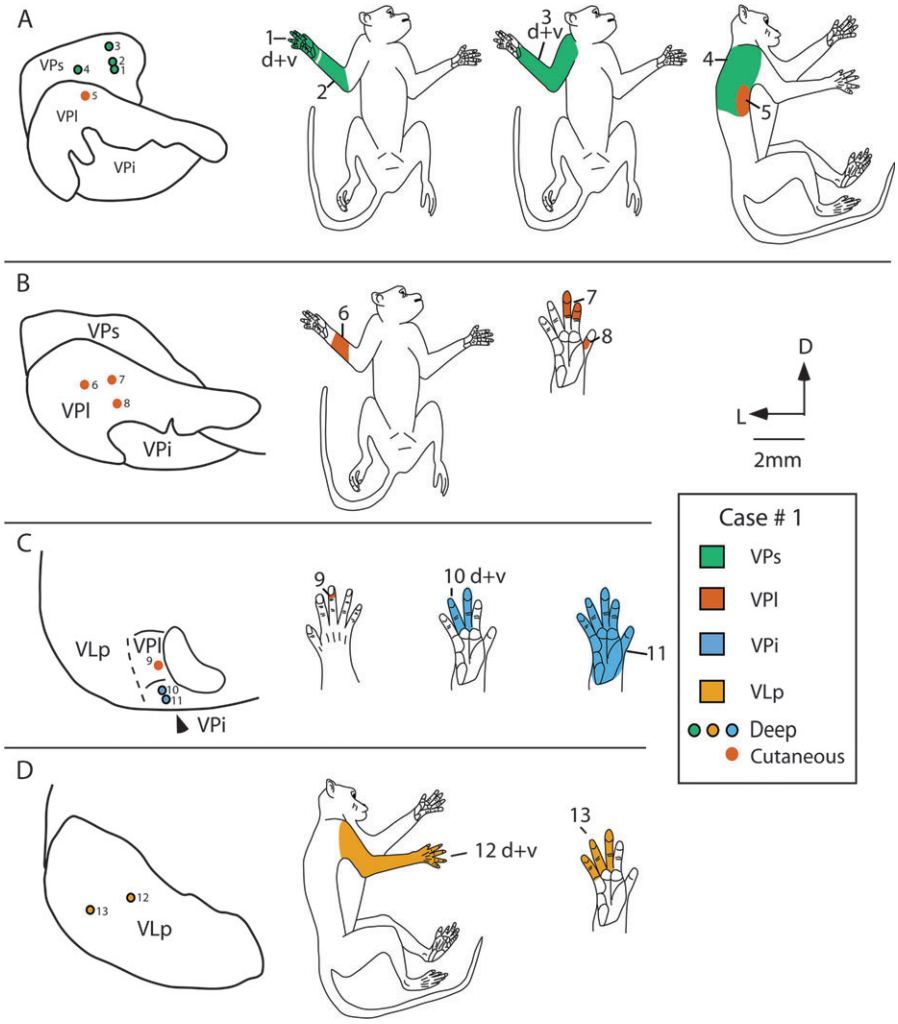

Figure 5. Recording site progressions for neurons through coronal sections of the thalamus in case #1 (*A–D*), and corresponding receptive fields for neurons at those sites (body part drawings on the right). Neurons in VPs had relatively large receptive fields that showed some smooth progressions on the forelimb (r.f. 1–4). As recording sites moved into VPl, neurons responded to cutaneous stimulation, receptive fields were relatively small, and a re-representation of the body was observed (r.f. 5–9). As recording sites moved into VPi, neurons responded to stimulation of deep receptors, receptive fields became larger, as in VPs, and a re-representation of body parts was observed (r.f. 10 and 11). Receptive fields for neurons rostral to VP, in VLp, were relatively large (e.g., r.f. 12) and neurons responded to stimulation of deep receptors. The distance between sections (*A*) and (*B*) is 150 μm, (*B*) and (*C*) is 350 μm, and (*C*) and (*D*) is 150 μm. See Table 1 for abbreviations. Conventions as in previous figures.

followed by the trunk and then the forelimb and hand. These representations of different body parts in VPs were just dorsal to similar representations in VPl. Medial to the digit representation was the representation of the nose (Fig. 4). Receptive fields for neurons in VPs were large compared with those for neurons in VP, but were similar in size when compared with receptive fields for neurons in VPi (Figs 5 and 6).

Examination of Nissl stained sections revealed that cell packing is less dense in VPs than VPl. Likewise, VPs stains moderately to darkly for CO and this staining is somewhat reduced from that of VPl. CB expression is low in both VPs and VPl, and VPs stains much like VPl for Cat-301. Thus, most of the borders of VPs are distinct, and when multiple stains are utilized and the entire series of sections is examined, VPs can be distinguished from VP (Fig. 3*C*,*D*).

Taken together, the data indicate that VP proper (VPl + VPm; Table 1) and VPi can be identified using both functional and architectonic criteria. Although the border between VPs and VPl was more difficult to determine than other borders, the architectonically defined border was consistent across cases and corresponded to this border described elsewhere (see Kaas 2008, for review). Further, the architectonic boundary between VPs and VPl matched precisely with the functionally defined border. Functional differences between these nuclei are best appreciated when results from dorsoventral progressions of recording sites through each nuclei are examined. Such an analysis demonstrates changes in receptive field size, re-representations of body parts, and differences in the modality of stimulation to which neurons respond (Figs 5 and 6). For example, in case no. 1 (Fig. 5), neurons in VPs respond to stimulation of deep receptors on the trunk (r.f. 4). With a dorsoventral progression of recording sites through VPs, receptive fields moved from the forelimb to the hand (r.f. 3-r.f. 1). As recording sites entered VPl, neurons responded to cutaneous stimulation, receptive fields for neurons were much smaller (compare r.f. 4 and 5 and r.f. 1 and 8), and there was

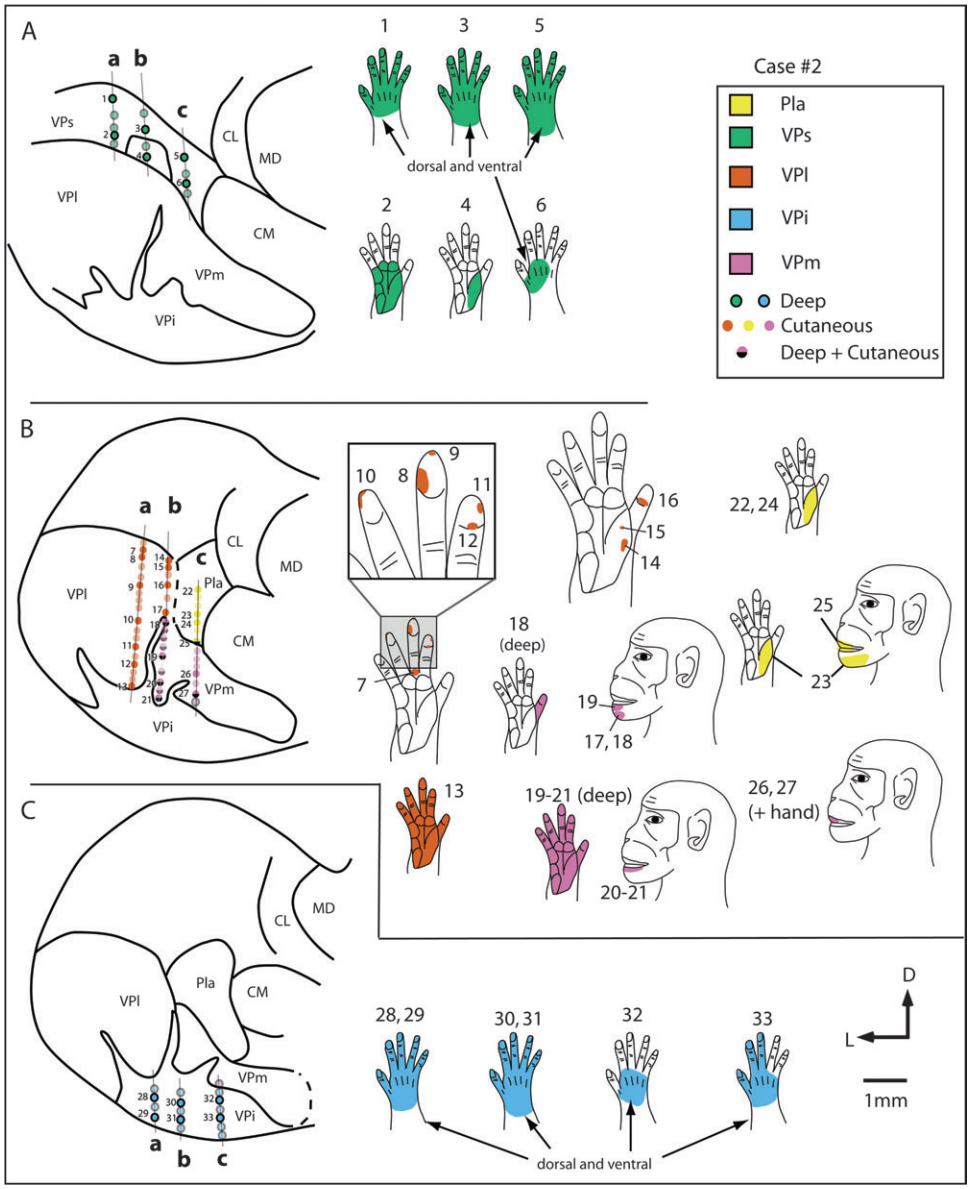

Figure 6. Recording site progressions for neurons through coronal sections of the thalamus in case #2 (*A–C*) in tracks a, b and c, and corresponding receptive fields for neurons at those sites (body part diagrams on the right). As in the previous case (Fig. 5) neurons in VPs (*A*) responded to stimulation of deep receptors and receptive fields on the hand (green) were large. As recording sites progressed ventrally, in VPl (orange) and VPm (pink; *B*) neurons responded to stimulation of cutaneous receptors on the contralateral hand and face, and receptive fields were much smaller. One electrode track (b) was at the border of VPm and the cell-sparse, fingerlike protrusion of VPi, and receptive fields at a number of sites were split (e.g., r.f. 18, 20, 21). Receptive fields on the face were small and neurons responded to cutaneous stimulation (in VPm), and receptive fields on the hand were large and neurons responded to stimulation of deep receptors (in finger-like extensions of VPi). The recording sites located in the most ventral portion of the dorsal thalamus, in VPi (blue; *C*), contained neurons that responded to stimulation of deep receptors and receptive fields for these neurons were relatively large and encompassed all or most of the hand (see blue r.f in *C*). In electrode track c, some recording sites were in Pla (yellow). Neurons here responded to stimulation of cutaneous receptors on the contralateral body, and receptive fields were on the face, hand, or both the face and the hand. Sections of the thalamus drawn on the left are composites of 4 sections each, and each composite covers 800 μm. See Table 1 for abbreviations. Conventions as in previous figures.

a re-representation of the dorsal trunk (r.f. 5), forelimb, and digits of the hand (r.f. 6–9). Recording sites in VPi revealed a reversal in the receptive field progression from the digits to the entire hand (r.f. 10 and 11), an enlargement of receptive field size, and a change in the submodality to which neurons respond (stimulation of deep inputs). Similar differences were observed in the second case in which receptive field progressions were analyzed through VPs, VP, and VPi (Fig. 6).

Other Nuclei

In both cases, recordings were made outside of the nuclei that compose the VP complex (see Table 1). In one case, responses were recorded in neurons just anterior to VP, in VLp (case no. 1), and in the other case neurons were recorded just dorsal to the posterior portion of VPm, in the anterior pulvinar (case no. 2). Neurons in VLp responded to stimulation of deep receptors, and receptive fields for neurons in VLp were large (Figs 4 and 5). Densely spaced recording sites revealed that VLp had

a gross topographic organization that was not as precise as that observed for VPl and VPm. Generally, the hindlimb was represented laterally, the forelimb and digits were represented medial to this, and portions of the face were represented most medially in the nucleus. In Nissl stained sections, VLp was composed of moderately packed cells. VLp was darkly staining for CO and moderately staining for Cat-301 and CB (not shown).

In case no. 2, a few recordings were made in the Pla (Fig. 6*B*, track c). Neurons in Pla responded to stimulation of cutaneous receptors on the contralateral hand and face, and receptive fields for neurons in Pla were relatively small in size. Receptive fields were larger than for neurons in VP, but smaller than receptive fields for neurons in VPs and VPi. Pla could be readily distinguished as a moderately stained nucleus using Nissl stains compared with the more darkly stained centre médian nucleus (CM) medially and VPm ventrally (Fig. 3*F*). In sections processed for CO, Pla was lightly stained, but was particularly distinct in sections stained for CB, where it stained very darkly compared with surrounding nuclei. In sections stained for Cat-301, Pla was lightly stained, and several moderately stained neurons were observed in the centre lateral nucleus (CL), as well as patchy neuropil staining that was light to moderate in intensity. No staining of CM or the lateral posterior nucleus (LP) was observed with Cat-301, and CM was unstained for CB (Fig. 3*D*).

Connections of Area 3b with Electrophysiologically Identified Locations in the Thalamus

Comparisons of the thalamocortical connections of the representations of different portions of the hand in area 3b were directly related to electrophysiologically identified locations in the dorsal thalamus. In case no. 1, an injection of FB was centered in the representation of the glabrous middle phalanx of D3 (mD3); an injection of DY was centered in the representation of the proximal thenar pad and an injection of FR was centered in the representation of dorsal digits 3–5. Ninety-five percent of all labeled cells in the thalamus were only labeled from a single injection in a particular cortical field, and 5% were double labeled; only 1 cell was triple labeled. The largest percentage of all labeled cells was in VPl, with sparser labeling in VPs, VPi, and VLp (Fig. 7). Injections in the mD3 representation resulted in labeled cell bodies in the electrophysiologically defined D3 representation in VPl. Labeled cells were also found in the representation of other digits in VPl (Fig. 8*B*,*C*). A few cells were observed in the chin representation of VPm. Because the injection site was small, and the D3 representation is several millimeters medial to the representation of the chin in area 3b, the few labeled cells observed in the chin representation of VPm are unlikely to be the result of spread of the injection into the chin representation of area 3b. A few labeled cells were observed in the forelimb representation of VPs and the hand representation of VPi (8B). The injection in the representation of the proximal thenar pad in area 3b was extremely small (~400 × 100 μm) and resulted in only a few labeled cells in the hand representation (including the glabrous pads) of VPl, and in the forelimb representation of VPs (Fig. 8*B*). Finally, a small injection into the representations of the dorsal hairy skin of D3-D5 in area 3b resulted in labeled cells in the representation of the digits and the upper trunk and shoulder representations of VPl (Fig. 8). Some labeled cells were in VPs in the representations of the hand, forelimb, and upper trunk. VPi also had a few labeled cells in the representation of the hand.

Double-labeled cells were observed in VPl from injections placed in the dorsal digits and thenar pad representations and from the mD3 and thenar pad representations.

Double-labeled cells were also observed in VPs from injections in the glabrous middle D3 representation and the dorsal digits representation (Fig. 8). Finally, one triple-labeled cell was observed in VPl from injections in each of the 3 representations. Together these data indicate that the representation of a portion of the hand in area 3b receives convergent input from 3 separate nuclei of the thalamus, as well as from different portions of the hand and forelimb representation within and across nuclei. Further, in a few instances, the same thalamic cells project to 2 or more functionally related representations of the hand.

Thalamocortical Connections of Somatotopically Matched Injections in Areas 3a, 3b, 1, and 2

Injections were placed in the 4 areas of anterior parietal cortex of 2 cases (Figs 9 and 10). In case no. 3 (Fig. 9), all injections were in cortical locations where neurons were responsive to touch or pressure on the distal glabrous phalanx of digit 4, or the phalanges of digits 4 and 3. Overall, the injections labeled somatotopically appropriate portions of the thalamic nuclei. In case no. 3, 98.5% of all cells were single labeled and 1.5% were double labeled. We could determine the representation in the thalamus that contained labeled cells because the protrusions of VPi into VP mark the border of the hand subnucleus with the face subnucleus (see above), and adjoining portions of VPs and VPi also represent the hand. However, the labeled neurons in the thalamus were somewhat more broadly distributed than expected by a precise somatotopic projection pattern. When neurons in the same nucleus were labeled by more than one injection, the clusters of labeled neurons projecting to different cortical areas overlapped, as expected from injections carefully placed in somatotopically matched regions of different areas. Some neurons in VPl were double-labeled, and projected to both areas 3b and 1, or area 3b and area 2. One neuron in VPs projected to areas 3b and 1.

The injection in area 3a resulted in labeled cells mostly in VPl and VLp (Figs 7 and 9). A few of these labeled neurons were in VPs, as expected for area 3a injections, but more were in VP. These 3a-projecting neurons were scattered over the dorsoventral extent of VPl, including the dorsal portion devoted to the representation of the arm and the middle to ventral portions devoted to the representation of the digits. Most of the labeled neurons were concentrated in the lateral portion of the hand subnucleus in VPl where digits 3–5 are represented. Many labeled neurons were observed far rostrally (Fig. 9*F*), in VLp or possibly a rostral extension of VPs. The injection in area 3b in case no. 3 labeled neurons predominantly in the hand subnucleus of VPl (Figs 7 and 9). Again, they were concentrated in the lateral portion of the subnucleus where digit 4 is represented, but the mediolateral spread of the labeled neurons likely included representations of other digits. The more dorsal labeled neurons in VPl likely involved proximal parts of the digits, the palm and other parts of the forelimb. A few labeled neurons were also observed in VPs and Pla. The injection in area 1 labeled neurons mainly in VPl, but a moderate number of

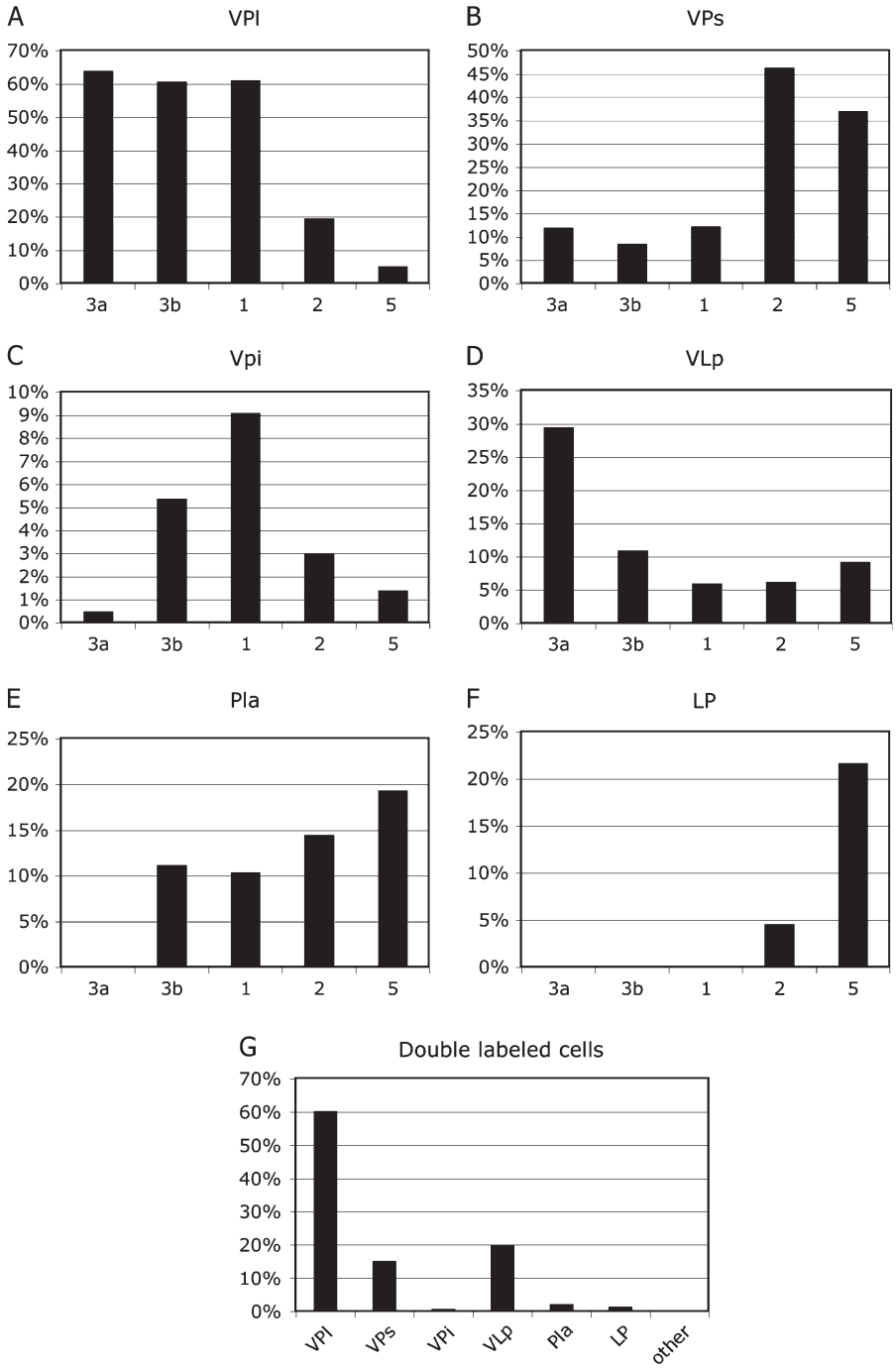

Figure 7. The average percentage of labeled neurons found in each thalamic nucleus following injections in areas 3a, 3b, 1, 2, and 5 (*A–F*). Percentages of neurons were determined for each area injected and then the mean percentage for that area from all cases was used to calculate the percentages shown in these histograms. Although multiple areas often receive input from the same nucleus, the density of input can vary. For example, VP projects to all 5 somotosensory areas, but with different densities. The percentage of double-labeled cells is shown in G. Most double-labeled cells—regardless of the 2 fields injected were found in VP. Of the double-labeled cells observed, VPs and VLp had smaller percentages. The scales (*y* axis) for each histogram shown here vary.

labeled neurons were also in VPi, VPs, and Pla. Finally, the injection in area 2 labeled neurons mainly in VPs with moderate labeling in VPl, and VPi in the location of the hand representation in each of these nuclei. These results indicated that each of the 4 areas of anterior parietal cortex receives somatotopically matched and mismatched input from more than one thalamic nucleus.

Results from case no. 4 (Fig. 10) were generally similar to those obtained from case no. 3. Again, injections were placed in somatotopically matched locations in areas 3a, 3b, 1, and 2. Each injection included cortex representing the distal phalanx of digit 3, whereas injections in areas 3a and 2 included neurons with larger receptive fields that extended to digits 2 and 4 (Fig. 10). Tracer leaked from the syringe for the area 3b

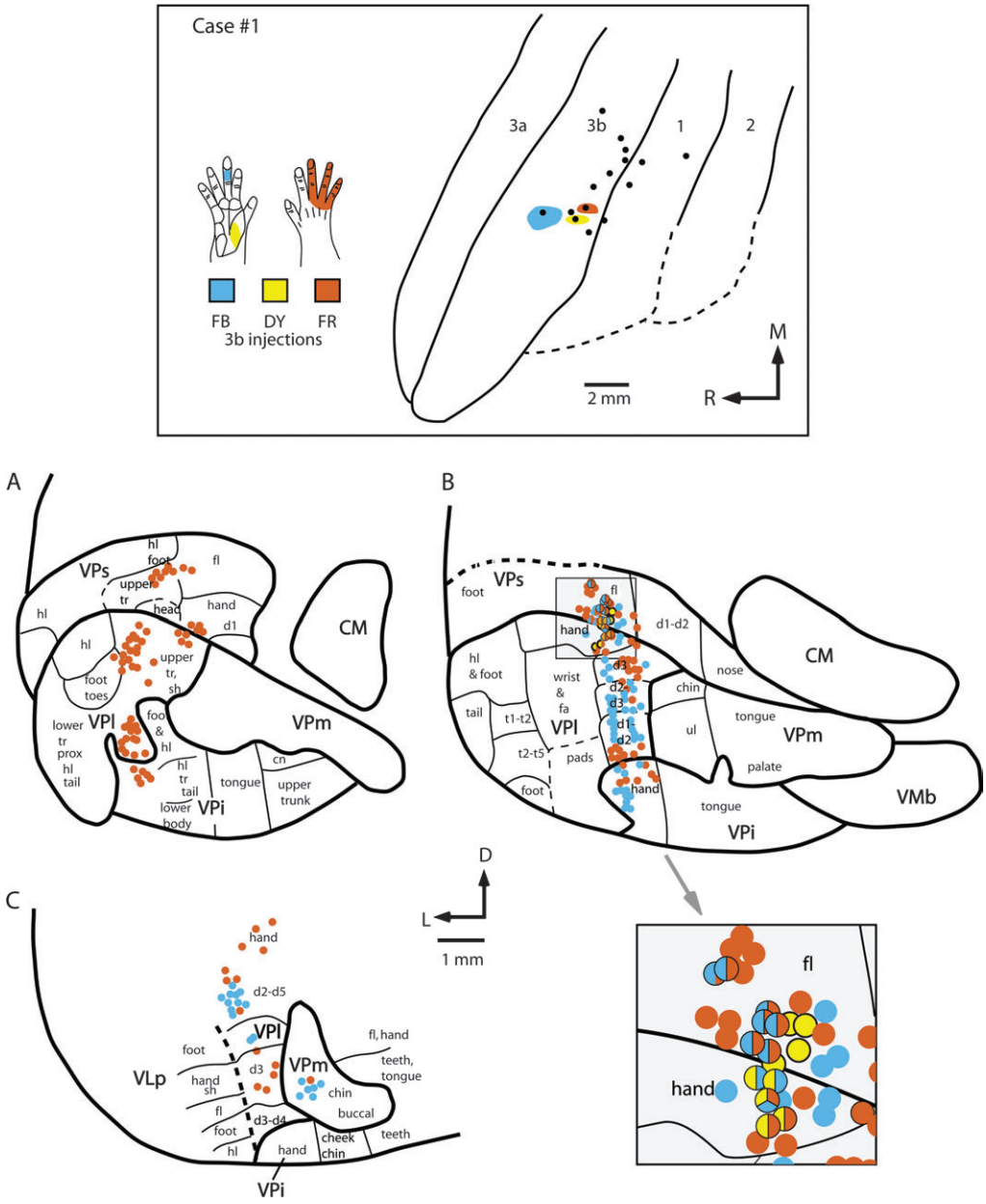

Figure 8. The location of electrophysiologically identified injections sites in area 3b in cortex that was sectioned tangentially (top box), and coronal sections of the thalamus (*A–C*) in case #1. In the top box, the receptive fields for neurons at the center of each injection site are drawn on illustrations of the hand and color coded to match the tracer injected. All injection sites are restricted to portions of the hand representation. The injection of FB was centered in the representation of glabrous middle D3, the injection of DY was centered in the representation of the proximal glabrous thenar pad, and the injection of FR was centered in the representation of the dorsal digits 3–5. Labeled cells resulting from these injections are depicted below and their direct relationship to electrophysiologically defined locations in the thalamus is depicted in sections *A–C*. These sections correspond to similarly labeled sections in Figure 4. These data indicate that a large amount of convergence is observed in thalamic projections to area 3b in that a given body part representation in area 3b, such as the middle glabrous D3, receives input not only from the same body part representation in VPl, but from other representations in VPl such as digit 2 and portions of the hand. Further, a few labeled cells were observed in the chin representation of VPm. Convergence is also observed across nuclei in that 3 separate nuclei (VPl, VPs, and VPi) project to a single location in area 3b. Finally, divergence is seen at the cellular level in that in some instances the same cells projected to 2 separate representations in area 3b. The large shaded box at the lower right of this figure is an enlarged image of the shaded square shown in B. Double- and triple-labeled cells in VPs and VPl are indicated by multicolored dots. See Table 1 for abbreviations. Conventions as in previous figures.

injection, so that both areas 3b and 1 contained portions of the injection site. In this case, 90% of cells were single labeled and 10% were double labeled and most of the double-labeled cells were in VPl (Fig. 7). As in the previous case, dorsoventral bands of neurons from all 4 injections occupied the hand subnucleus of VPl and adjoining parts of VPs. The area 3a injection labeled neurons in both VPl and VPs, and at rostral levels labeled neurons were in VLp (not shown). The labeled neurons in VPl extended from dorsal (Fig. 10*A*) to ventral (Fig. 10*C*) in the hand subnucleus. The area 3b plus area 1 injection labeled neurons throughout the hand subnucleus of VPl, a few neurons in adjoining nuclei VPs and VPi, and neurons in Pla. Some scattered neurons were observed at rostral levels at VPl/VLp border (not shown). The area 1 injection labeled neurons

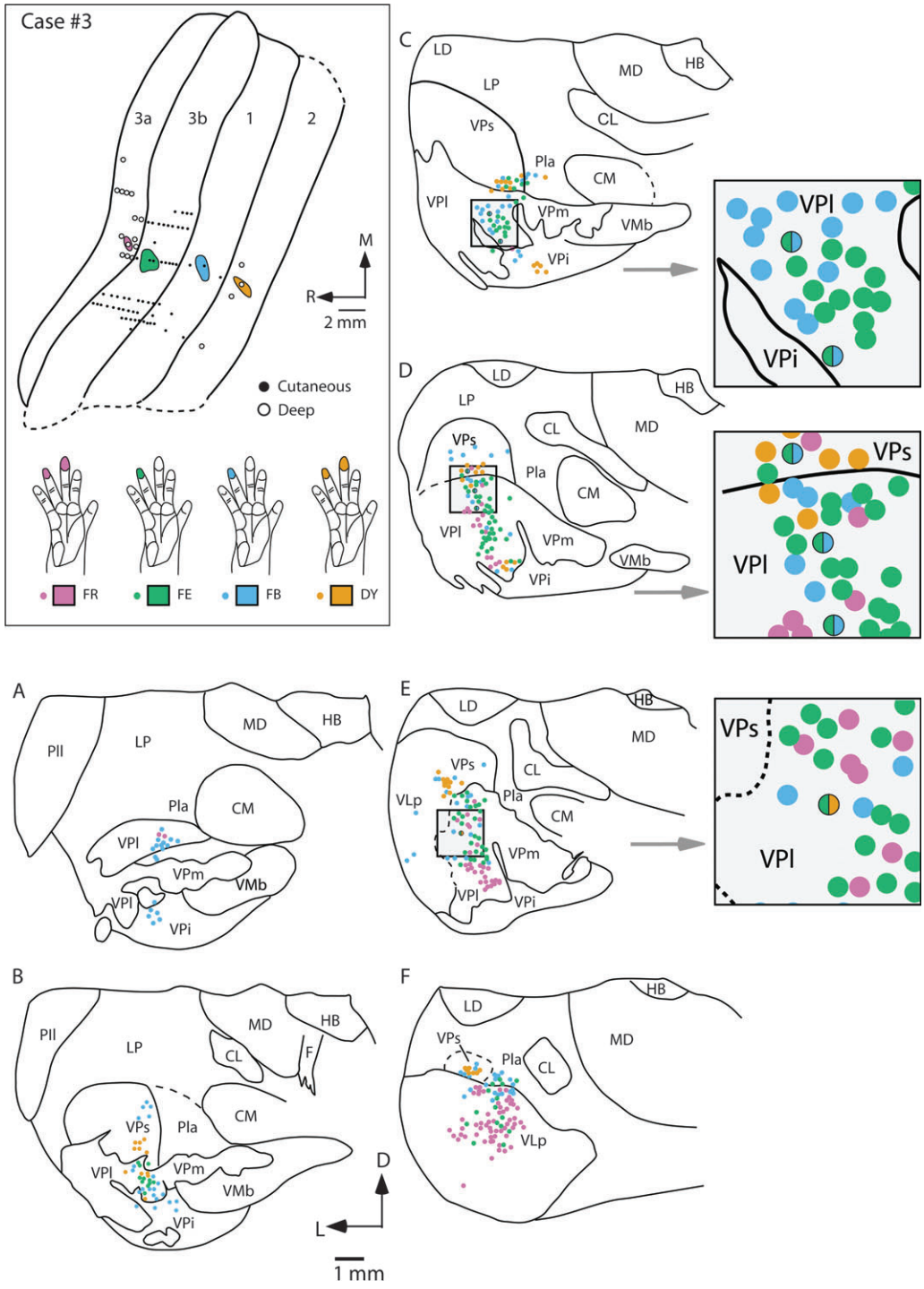

Figure 9. The locations of electrophysiologically identified injection sites in areas 3a, 3b, 1, and 2 in cortex that was sectioned tangentially (top left box), and coronal sections of the thalamus (*A–F*) in case no. 3. In the top left box the receptive fields for neurons at the center of each injection site are drawn on illustrations of the hand and color coded to match the area injected. Injections were centered in the representation of distal D4 in areas 3b and 1, and distal D3 and D4 in areas 3a and 2. Labeled cells resulting from injections in areas 1 and 2 were observed primarily in VPl, with moderate label in VPs. The injection in area 3a resulted in dense label in VLp and VPl. The injection in area 2 resulted in dense label in VPs and moderate label in VPl and VPi. In some instances double-labeled cells were observed in VPl and VPs from injections in areas 3b and 1 (grey boxes to the right). One double-labeled cell was observed in VPl from injections in areas 3b and 2. Solid lines in (*A–F*) mark architectonic boundaries of thalamic nuclei, and dashed line mark approximate boundaries. Sections are shown in a caudal (*A*) through rostral (*F*) progression. These sections are spaced by 150 μm. Abbreviations in Table 1. Conventions as in previous figures.

mainly in VPl and moderately labeled cells in Pla, VPi, and VPs. The larger injection in area 2 labeled many neurons in VPs and VPl, and a few in rostral Pla and in VLp (not shown). The majority of double-labeled neurons (38%) were the result of the injection in area 2 and either 3a, 3b, or 1. This is not surprising because the injection in area 2 was relatively large

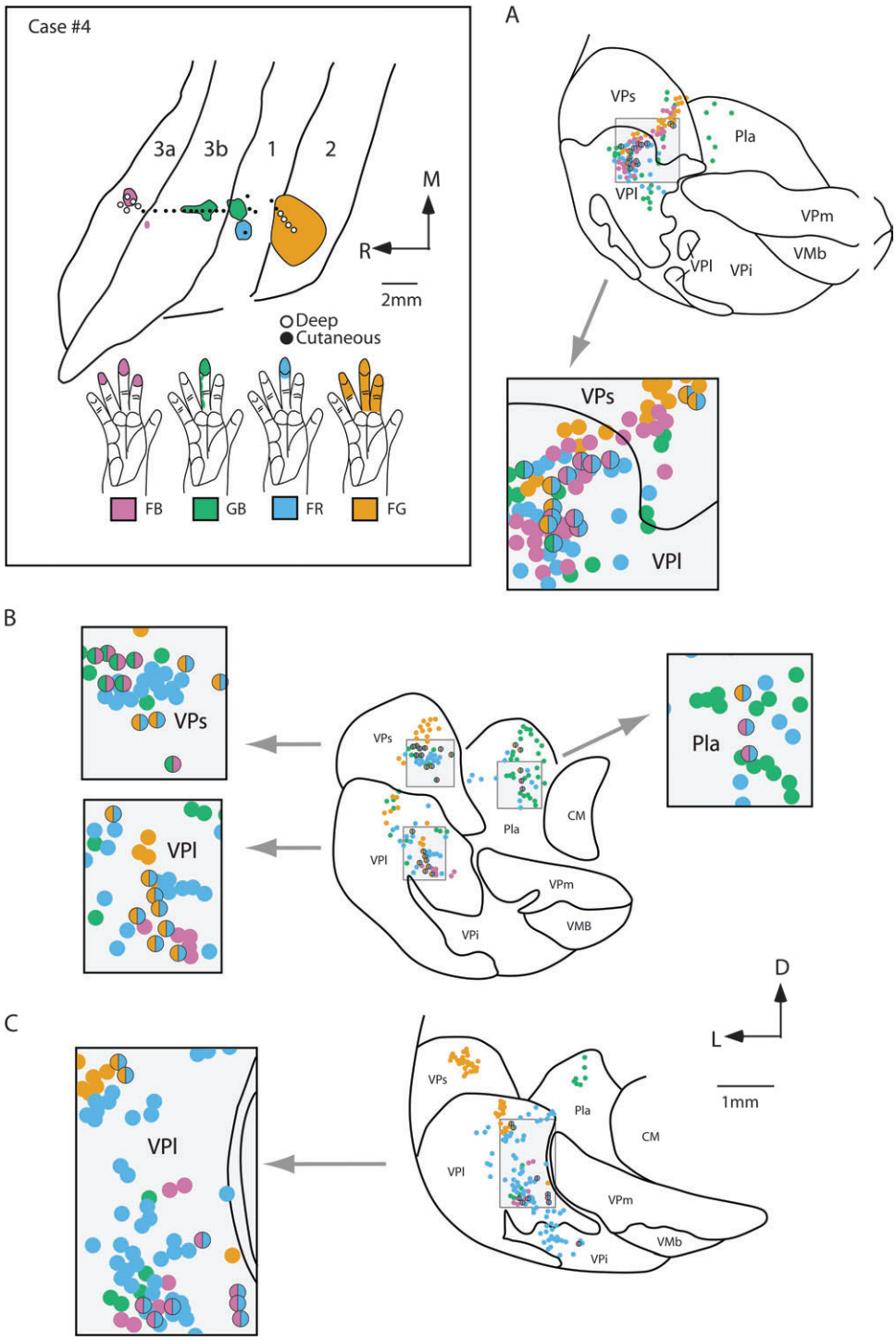

Figure 10. The locations of electrophysiologically identified injection sites in areas 3a, 3b, 1, and 2 in cortex that was sectioned tangentially (top left box), and coronal sections of the thalamus (*A–C*) in case no. 4. In the top left box the receptive fields for neurons at the center of each injection site are drawn on illustrations of the hand and color coded to match the area injected. Injections were centered in the representation of distal D3 in areas 3b and 1, and in D2–4 in areas 3a and 2. Patterns of label were similar to those described in case no. 3 (Fig. 8). The injection in area 2 resulted in dense label in VPs, and moderate label in VPl. The injection in area 3a resulted in label in VPl, VPs, and VLp (on rostral sections not shown). In some instances double-labeled cells were observed (grey boxes) in VPl, VPs, and Pla. The distance between sections (*A*) and (*B*) is 1400 μm, and between (*B*) and (*C*) is 1600 μm. Abbreviations in Table 1. Conventions as in previous figures.

and likely included multiple portions of the hand representation. Thus, the injection in area 2 was more likely to be topographically matched with the injections in the other fields. Most of the double-labeled cells that were observed in this case were in VPl (Fig. 7*G*). Only 3 of the double-labeled neurons in VP were from the area 3b and 1 injections suggesting that although the injection in 3b spread slightly into area 1, it did not contaminate the injection site in area 1. Some neurons in

VPl were also labeled by the area 3b and the area 2 injections (Fig. 11*A–C*). Other neurons in VPl were labeled by both the area 1 and the area 2 injections, or by the area 3a and the area 1 injections (Fig. 11*D–F*). Cells labeled by both the area 3a and the 3b injection or the area 1 and the area 2 injections were found in VPs and VLp. A few double-labeled cells from both the area 3a and the area 1, or the area 1 and the area 2 injections were in Pla.

Taken together, these data indicate that VPl projects to all 4 anterior parietal cortical areas but with different densities (Fig. 7*A*). Further, projections from VPl to these fields are from overlapping groups of neurons corresponding to the overlapping somatotopic locations of the injection site. However, the spread of label in VP from injections from all 4 fields indicates that mismatched, but functionally related body part representations projected to a single location in each field. In addition, other nuclei such as VPs, VPi, and VLp also project to all 4 fields, but with different densities (Fig. 7*B–D*). Thus, rather than finding a one-to-one correspondence between a cortical field and a thalamic nucleus, somatosensory areas in anterior parietal cortex are defined by a high degree of divergence from a single nucleus to multiple fields, as well as a high degree of convergent inputs from a number of thalamic nuclei to a single field, and these connections are somatotopically matched and mismatched.

Comparisons of Thalamocortical Connections of Areas 2 and 5

In the present study we also placed injections in separate but functionally related representations in area 2 to determine if thalamic projections to area 2 are divergent. In another set of experiments we placed injections in somatotopically congruent locations in both areas 2 and 5 to directly compare thalamic projections to these 2 areas in the same animals. Eight injections were placed in portions of the hand representation in area 2 in 7 cases (Table 2; case no. 9 not shown) and 4 injections were placed in portions of the hand representation in area 5 in 4 cases. In one of the cases illustrated, 2 injections were placed in area 2, one in the D1 representation and the second in the D2 representation (case no. 5 Figs 12 and 13). Areas 2 and 5 were identified using electrophysiological criteria combined with architectonic criteria as described by Pons et al. (1985). Briefly, area 2 is characterized by dense and relatively thick layers IV and VI. The architectonic boundary of area 2 and 5 is not as distinct as that of the area 1/2 boundary, but generally can be distinguished by a decreased thickness and

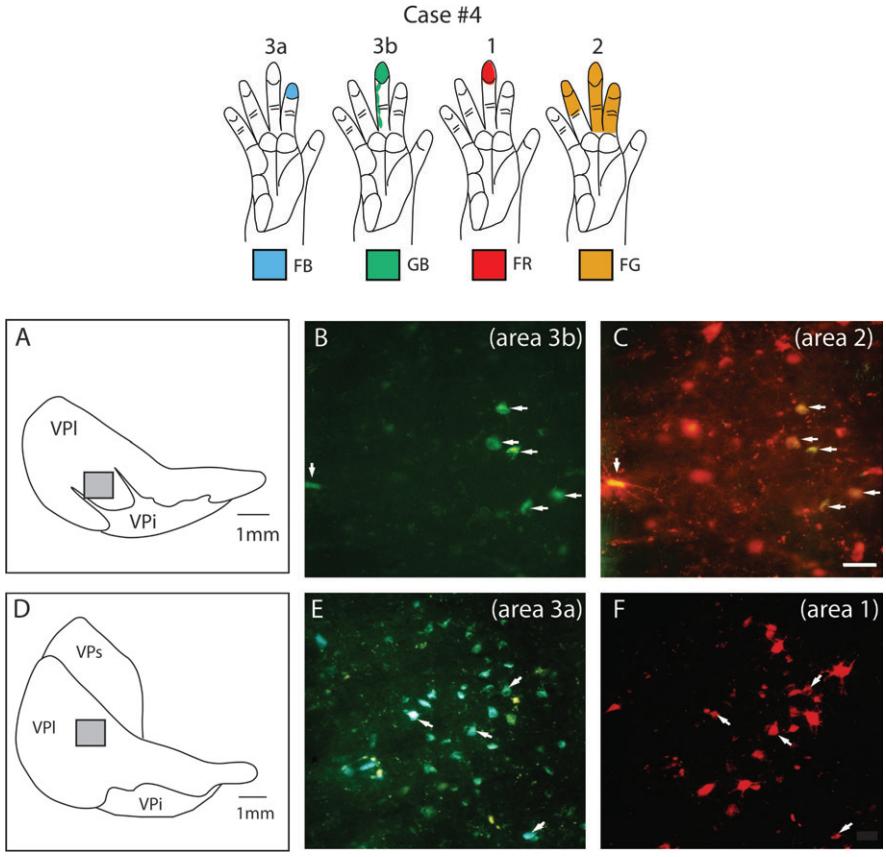

Figure 11. Photomicrographs of coronally sectioned portions of the dorsal thalamus that contain double-labeled cells (*B*, *C*, *E*, and *F*) resulting from injections into electrophysiologically defined locations in areas 3a, 3b, 1, and 2 in case no. 4. The illustration at the top depicts the receptive field locations for neurons at the center of each injection site. In this figure only, the color of the receptive field corresponds to the color of the fluorescing labeled cell bodies, rather than to the area injected. The precise location of these cells in VPl is illustrated in (*A*) and (*D*) (shaded box). Double-labeled cells (white arrows in *B* and *C*) were observed in VPl following injections of fluorescent GB in area 3b and FG in area 2. Double-labeled cells were also observed in VPl following injections of FB in area 3a and FR in area 1. These photographs were taken from sections intervening between those reconstructed in Figures 9 and 10 from this same case. Scale bar for photographs = 100 μm. See Table 1 for abbreviations. Conventions as in previous figures.

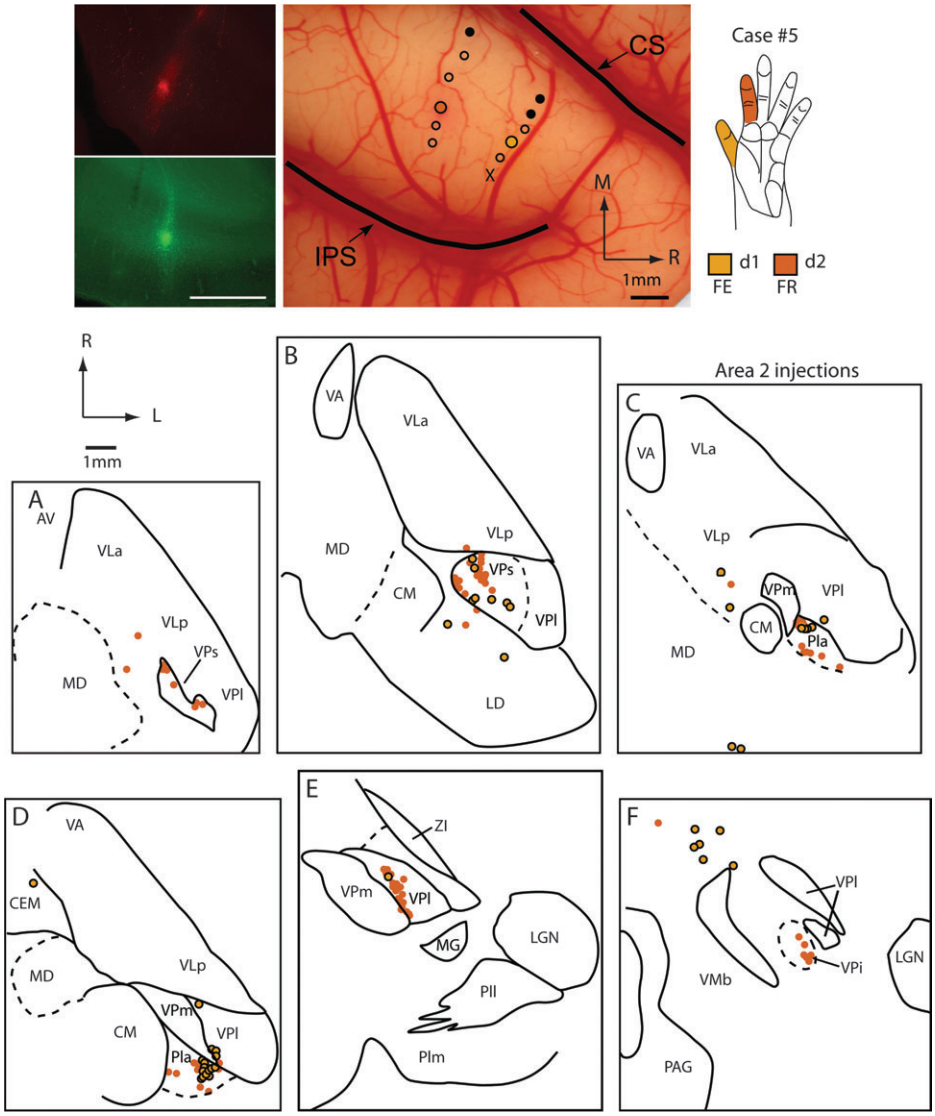

Figure 12. Digital images of injections of FR (red) into the representation of glabrous digit 2 and FE (green) into the representation of glabrous digit 1 in area 2 (top left panel). The locations of injection sites for this case (no. 5) were placed in electrophysiologically defined locations in area 2 that are shown on a digital image of the exposed cortex in the middle top panel, and receptive fields for the neurons at these injection sites are shown in the top right panel. Labeled cell bodies resulting from those injections are depicted in horizontal sections of the thalamus (*A–F*). As in cases no. 3 and 4 (Figs 8 and 9), projections to area 2 were observed from VPs and Pla, with moderate projections from VPl and VPi. Thalamic sections are 640 μm apart. Abbreviations in Table 1. Conventions as in previous figures.

density in layer IV and a decreased density of neurons in layer VI. Further, under our recording conditions, the response of neurons fell off dramatically in area 5 compared with area 2 and the amplitude of the stimulus needed to elicit a response was generally greater in area 5 than in area 2.

The densest projections to area 2 were from VPs with moderate projections from VPl, Pla, and LP (Fig. 7). In case no. 5 in which different representations in area 2 were injected, label in VPs and Pla overlapped in some regions but was in separate locations in other regions (Figs 12 and 13). Thus, partially overlapping populations of cells in VPs and Pla project to the representations of adjoining digits in area 2, demonstrating at least a moderate amount of somatotopically mismatched projections that could account for a modest amount of cortical reorganization after limited sensory loss.

Injections placed in both area 2 and area 5 in similar representations (e.g., Fig. 14), or portions of the hand representation (Figs 15 and 16), indicate that they receive inputs from overlapping populations of thalamic neurons. In case no. 6, an injection was placed in a part of area 2 responsive to touch on the distal phalanx of digit 1, and a second injection was placed in a part of area 5 where touch over all of the glabrous digit 1 activated neurons (Fig. 14). The injections labeled overlapping groups of neurons in VPs and Pla (Fig. 14*C–E*). Neurons were also labeled ventrally along the medial margin of VPl, within the digit 1 representation. There were many neurons in LP that were labeled from the area 5 injections and fewer neurons in LP were labeled from the area 2 injection. Results were similar in case no. 7 where injections were placed in adjoining portions of the hand representation of areas 2 and 5 (Fig. 15). In this case, the clusters of labeled cells in the thalamus overlapped only slightly, and the number of labeled cells for the small area 2 injection was much less than for the area 5 (Fig. 15). Nevertheless, both injections labeled neurons

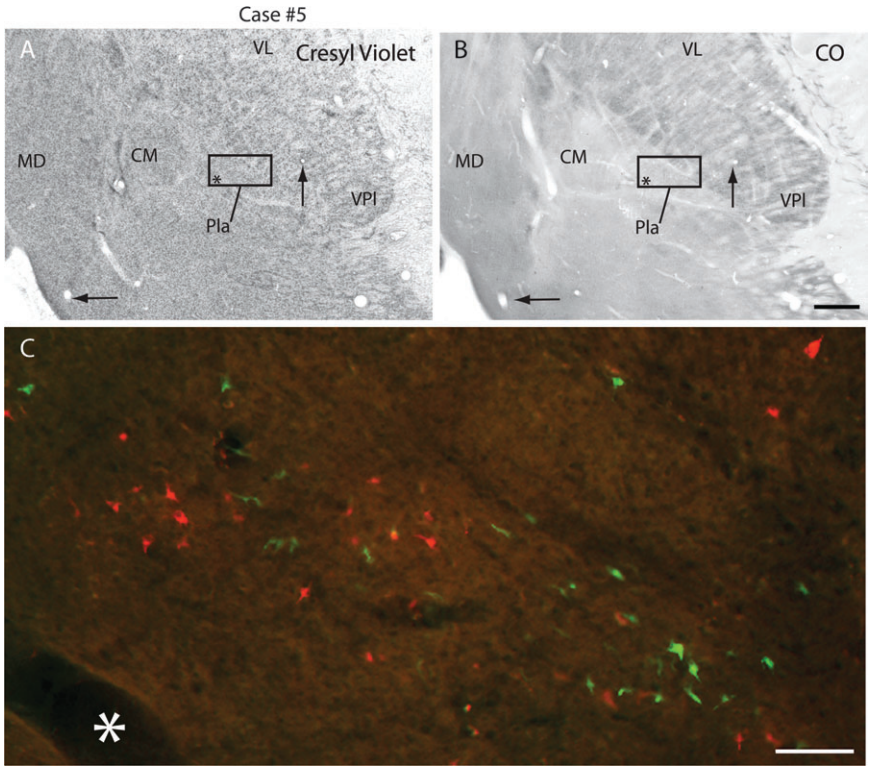

Figure 13. Digital images of horizontal sections stained with Cresyl violet (*A*) and reacted for CO (*B*) in case #5, and labeled cells in Pla (*C*) resulting from injections in D1 (FE, green) and D2 (FR, red). The box in (*A*) and (*B*) indicates the location of the cells depicted in C. The asterisk marks the same blood vessels in the 3 images. Scale bar = 1mm for (*A*) and (*B*) and = 100 μm in (*C*). See Table 1 for abbreviations. Conventions as in previous figures.

in VPs. Injections in area 5 also resulted in a large number of labeled cells Pla and LP and sparse labeling in CL and the mediodorsal nucleus (MD). In case no. 8 in which nonadjacent representations of the hand were injected (distal d1 for the area 2 injection and the hypothenar pad + forearm taps for the area 5 injection), labeled cells from both injections partially overlapped in VPs and Pla. As in the previous case injections in area 5 also resulted in dense labeling in LP and the LP/VLp border, and moderate to sparse labeling in VPl, CL, and MD (Fig. 16). A final case (no. 9 not shown) in which injections in area 2 and area 5 were made without electrophysiological guidance resulted in patterns of label that were remarkably similar to those described for case no. 8.

When all cases of area 2 and 5 injections are considered together, the data indicate that VPs is consistently and densely labeled following injections in area 2, and that Pla and VPl are moderately labeled in most cases. On the other hand, area 5 is characterized by dense inputs from VPs, LP, and Pla, and very sparse inputs from VPl (Fig. 7). As with the comparisons of thalamocortical connections described in the previous section, areas 2 and 5 have a high degree of convergent and divergent inputs.

Discussion

The present results demonstrate that there are 4 topographically organized representations of receptors of the skin, or muscle and joints in nuclei in the dorsal thalamus that have distinct architectonic appearances and patterns of connectivity with anterior and posterior parietal somatosensory areas of the cortex. These nuclei project in different combinations and with different densities to cortical areas 3a, 3b, 1, 2, and 5 (Fig. 17). In the following discussion, we focus on previous studies of connections using neuroanatomical tracing techniques rather than studies using lesion/degeneration techniques because in the latter type of study, the lesion most often encompassed more than a single field, and these studies are confounded because fibers of passage are often included in the lesion.

Somatosensory Nuclei of the Thalamus

The somatosensory thalamus receives inputs from both the lemniscal and spinothalamic pathways. Afferents from rapidly and slowly adapting mechanosensory receptors of the skin ultimately terminate in the gracile and cuneate nuclei of the brainstem and travel via the medial lemniscus to the contralateral VPm and VPl, respectively. Afferents from muscle spindles ultimately terminate in the external cuneate nucleus and project via the medial lemniscus to the contralateral VPs (See Kaas 2008, for review). Finally, spinothalamic input carrying information from wide dynamic range neurons in Lamina 5 and nociceptive, thermoceptive, and other neurons associated with introception in lamina 1 project to VPi as does the spinal trigeminal nuclei (Craig and Zhang 2006).

The topographic organization and neural response properties of the ventral posterior nucleus have been described previously in macaque monkeys (e.g., Mountcastle and Henneman 1952; Poggio and Mountcastle 1963; Loe et al. 1977; Jones and Friedman 1982; Rausell and Jones 1991) and squirrel monkeys

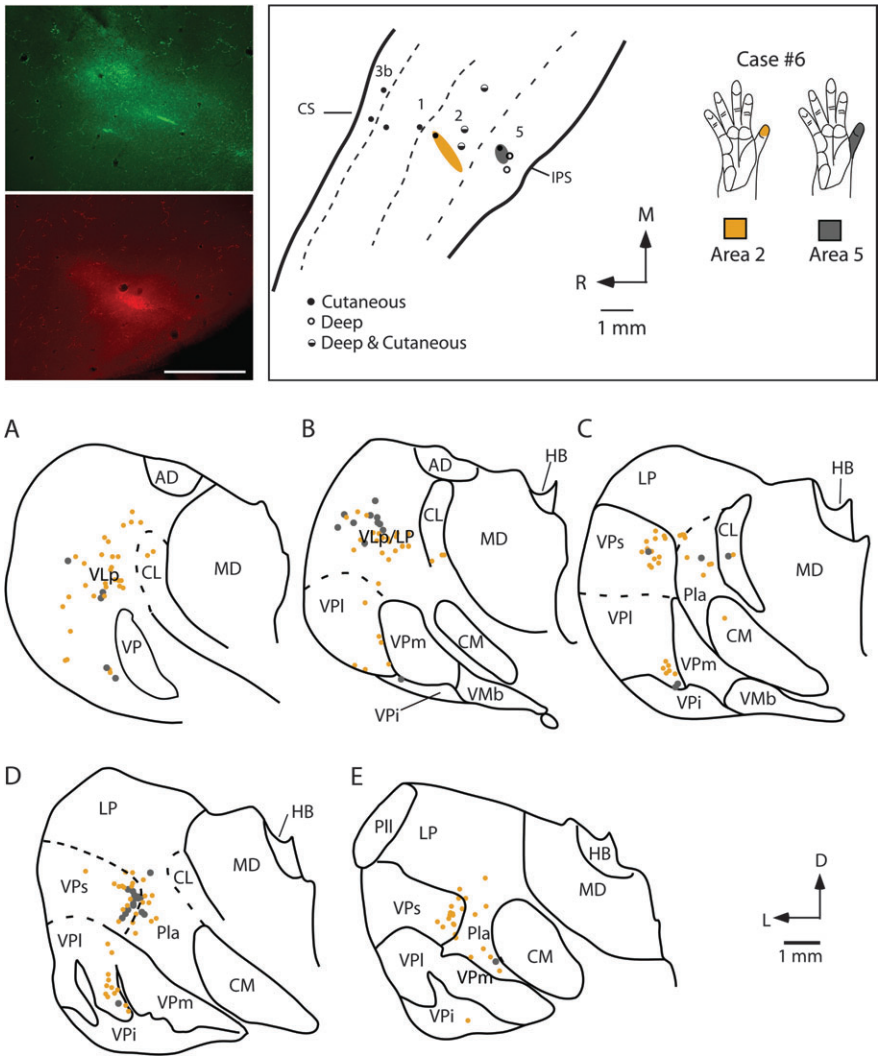

Figure 14. Digital images of an injection of FE (green) placed in the representation of glabrous distal digit 1 of area 2 and an injection of FR (red) placed in the D1 representation of area 5 (top left panel). Electrophysiological recording sites for this case (case no. 6) are illustrated in the top middle panel and receptive field locations for neurons at each injection site are drawn in the top right panel. Labeled cell bodies resulting from those injections are drawn in coronal sections through the thalamus in (*A–E*). As in cases no. 3, 4, and 5 (Figs 8, 9, and 12), projections to area 2 were observed from VPs, VPl, and Pla. Labeled cells were also observed in VLp. The injection in area 5 was very small and resulted in labeled cells in VPs, Pla, and LP. Sections are 400 μm apart. Abbreviations in Table 1. Conventions as in previous figures.

(e.g., Kaas et al. 1984; see Kaas 2008, for review). Results from the present investigation are consistent with results from previous studies in several ways. First, in previous studies, neurons in VPl and VPm respond to cutaneous stimulation of the contralateral body and face, respectively. Second, representations of the tail, hindlimb, and forelimb in VPl form a lateromedial progression and representations of the chin, lips and oral structures in VPm form a lateromedial progression. Third, receptive fields for neurons in VP are small, and the topographic organization is very detailed. Finally, VP has a unique architectonic appearance, and contains septal discontinuities that separate representations of different body parts that can be identified in CO and other histological preparations (see Kaas 2008, for review).

The somatotopic organizations of VPs and VLp have not been determined in any detail in previous studies in primates. They have been identified architectonically, and limited recordings suggest that these nuclei parallel VP in somatotopic organization (e.g., Dykes et al. 1981; Kaas et al. 1984; Kaas 2008, for review). Previous neuroanatomical studies of VPs (e.g., Pons and Kaas 1985b) and VLp (Craig 2008; Evrard and Craig 2008) support the conclusion that these nuclei represent the contralateral body from face to hindlimb in a mediolateral sequence (see Kaas 2008, for review). Dorsal and rostral shell regions of VP, in the locations of VPs and VLp, respectively, have been described previously in electrophysiological recording studies and a number of different terminologies have been used to refer to these thalamic regions (e.g., Poggio and Mountcastle 1963; Loe et al. 1977; Jones and Friedman 1982; Jones et al. 1982; see Macchi and Jones 1997; Kaas 2008, for review). Neurons in these regions respond to stimulation of deep receptors of the contralateral body and face. Although we found a few sites in the dorsal portion of VP in which neurons responded to deep stimulation, this was distinct from the neurons just dorsal to VP that responded to stimulation of deep receptors. We believe that most of the dorsal shell region of previous studies corresponds to VPs of the present study, and the rostral shell region corresponds to part of VLp (see Kaas

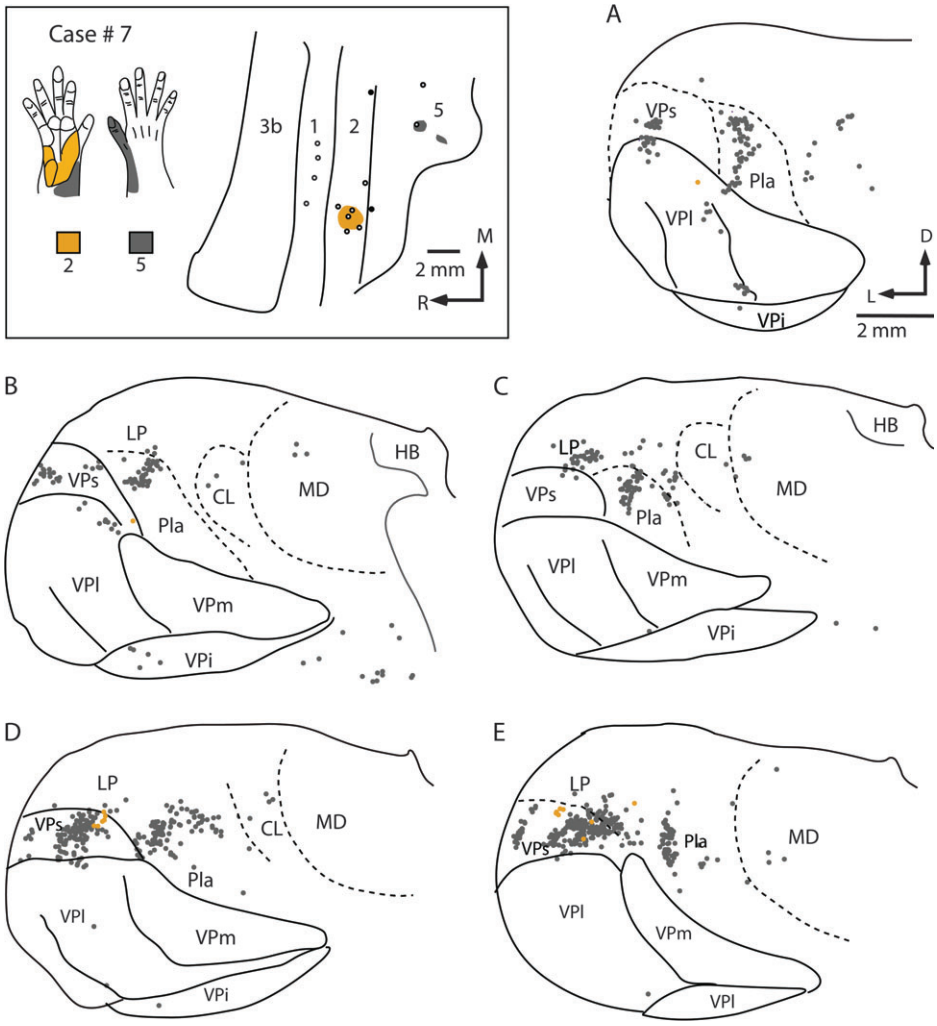

Figure 15. The location of injection sites placed into electrophysiologically defined locations in areas 2 and 5 in case no. 7 (box at top left) and labeled cell bodies resulting from the injections in a coronal series through the thalamus (A–E). An injection of DY was centered in the proximal palm representation of area 2 and an injection of CTB was centered in radial hand, wrist and dorsal d1 of area 5. Labeled cells resulting from injections in area 2 were observed almost exclusively in VPs. Injections in area 5 resulted in labeled cells in VPs, Pla, LP, and VLp with sparse label in CL and MD. Sections are 400 μm apart. Abbreviations in Table 1. Conventions as in previous figures.

2008). Both VPs and VLp contain neurons that responded to muscle manipulation and joint movements and rotations. Further, both are architectonically distinct (Fig. 3) and have different patterns of interconnection with the neocortex. Thus, VLp (VPLo) has dense projections to motor and premotor areas and to area 3a (see Wiesendanger and Miles 1982; Macchi and Jones 1997; see Fang et al. 2006, for review), whereas VPs has major projections to areas 2 and 5 (Pons and Kaas 1985b). For these reasons, it is more consistent with other nomenclature to refer to VPs and VLp as separate nuclei rather than as a shell of VP proper (Table 1). Although it is possible that VPs and VLp are actually a part of the same irregularly shaped nucleus that partially encapsulates VPl, we think this is unlikely because VLp receives inputs from the deep cerebellar nuclei (e.g., Stepniewska et al. 2003; Evrard and Craig 2008), VPs receives inputs from muscle spindle afferents via the medial lemniscus (Wiesendanger and Miles 1982) and each has a distinct pattern of thalamocortical connections.

We also found evidence for a representation of receptors of the skin and muscles of the contralateral body in a nucleus just ventral to VP, in VPi. The major activating inputs to VPi are from the wide dynamic range and other neurons of the spinothalamic tract (e.g., Craig and Zhang 2006). Although VPi had relatively sparse projections to anterior parietal areas and posterior parietal area 5, it has major cortical projections to higher order somatosensory areas of the lateral sulcus, such as S2 and PV (Friedman and Murray 1986; Krubitzer and Kaas 1992; Disbrow et al. 2002; Qi et al. 2002; Coq et al. 2004). Finally, in the one case that had a few recording sites in Pla, neurons responded to low threshold cutaneous stimulation of the contralateral body. The anterior pulvinar has not been systematically explored with microelectrode recordings, but an early investigation by Loe and colleagues (1977) in which VP and surrounding nuclei were studied provided limited evidence that Pla (Pul.o) contains neurons responsive to cutaneous stimulation of the contralateral limbs. There is some evidence that Pla receives some input from the deep layers of the superior colliculus, which are associated with somatosensory processing (see Jones 2007). However, it appears that much of the activating inputs to Pla may be from area 2 and other areas of somatosensory cortex to which it also projects (see Kaas 2008). Because of these broad reciprocal

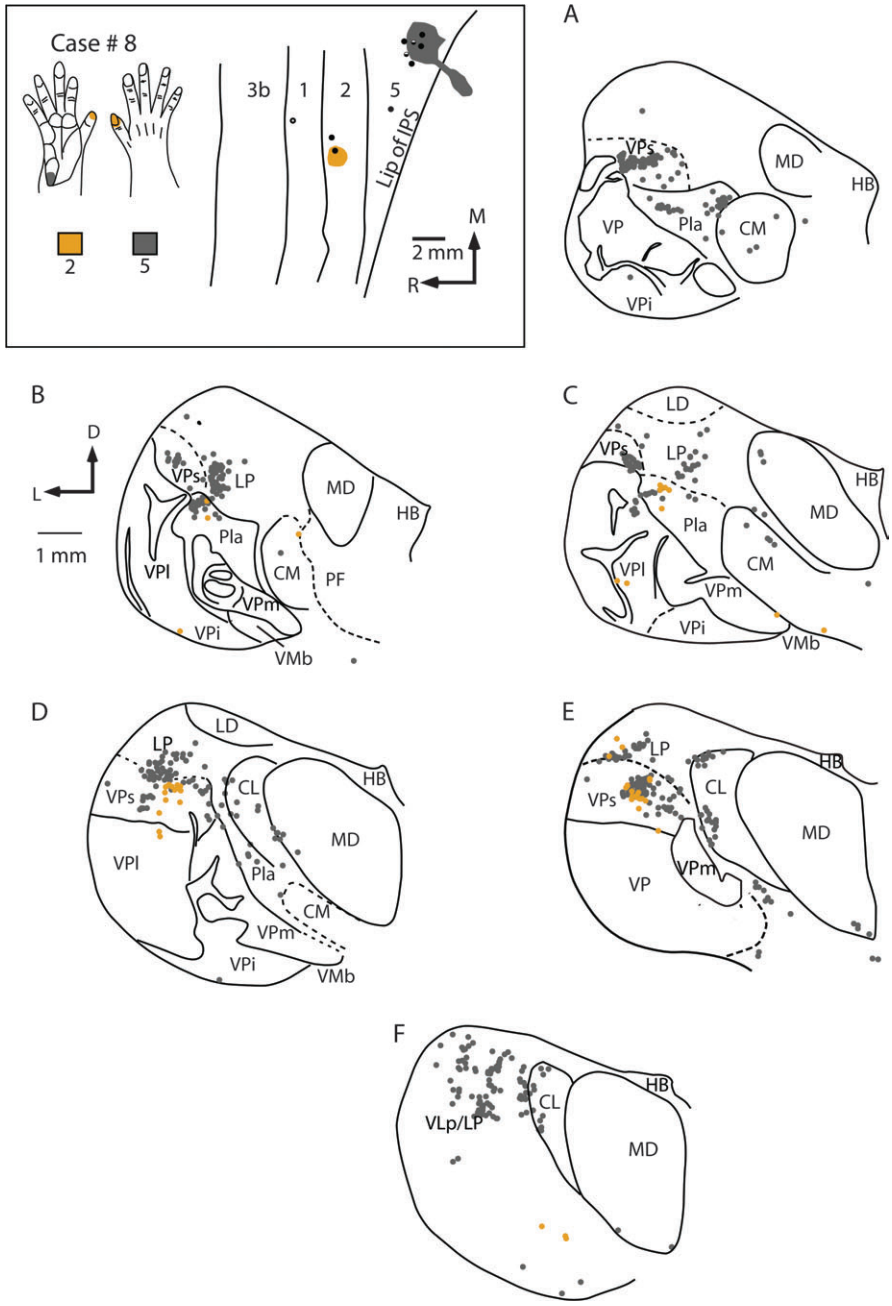

Figure 16. The location of injection sites placed into electrophysiologically defined locations in areas 2 and 5 in case #8 (box at top left) and labeled cell bodies resulting from these injections in a coronal series through the thalamus (*A–F*). An injection of DY was centered in the representation of the tip of area 2 and an injection of CTB was centered in representation of the proximal hypothenar pad of area 5. Labeled cells resulting from injections in area 2 were observed in VPs, and Pla, with moderate label in VPl. Injections in area 5 resulted in labeled cells in VPs, Pla, LP, and VLp with sparse to moderate label in CL and MD. Thalamic sections are 600 μm apart except for (*C*) and (*D*) that are 1200 μm apart. Abbreviations in Table 1. Conventions as in previous figures.

connections with a number of regions of cortex, it has been proposed that Pla coordinates activity across many cortical areas (Sherman and Guillery 2006).

Taken together, both the present study and previous studies indicate that there are at least 4 and possibly 5 nuclei in the thalamus associated with somatosensory processing. This is much like the visual system in which several nuclei in the thalamus are associated with visual processing, but the number of these thalamic nuclei is distinctly smaller than the vast array of sensory fields in the cortex. One defining feature of a particular cortical field would be its unique patterns of input from a combination of nuclei in the thalamus that project with different magnitudes (Figs 7 and 17). This type of processing network would allow many degrees of freedom for combining submodalities of inputs to generate complex perceptual representations of the highly dynamic sensory environment.

Thalamic Connections with Anterior Parietal Fields

Our results on thalamocortical connections are consistent with those of a number of previous studies. Here we review data

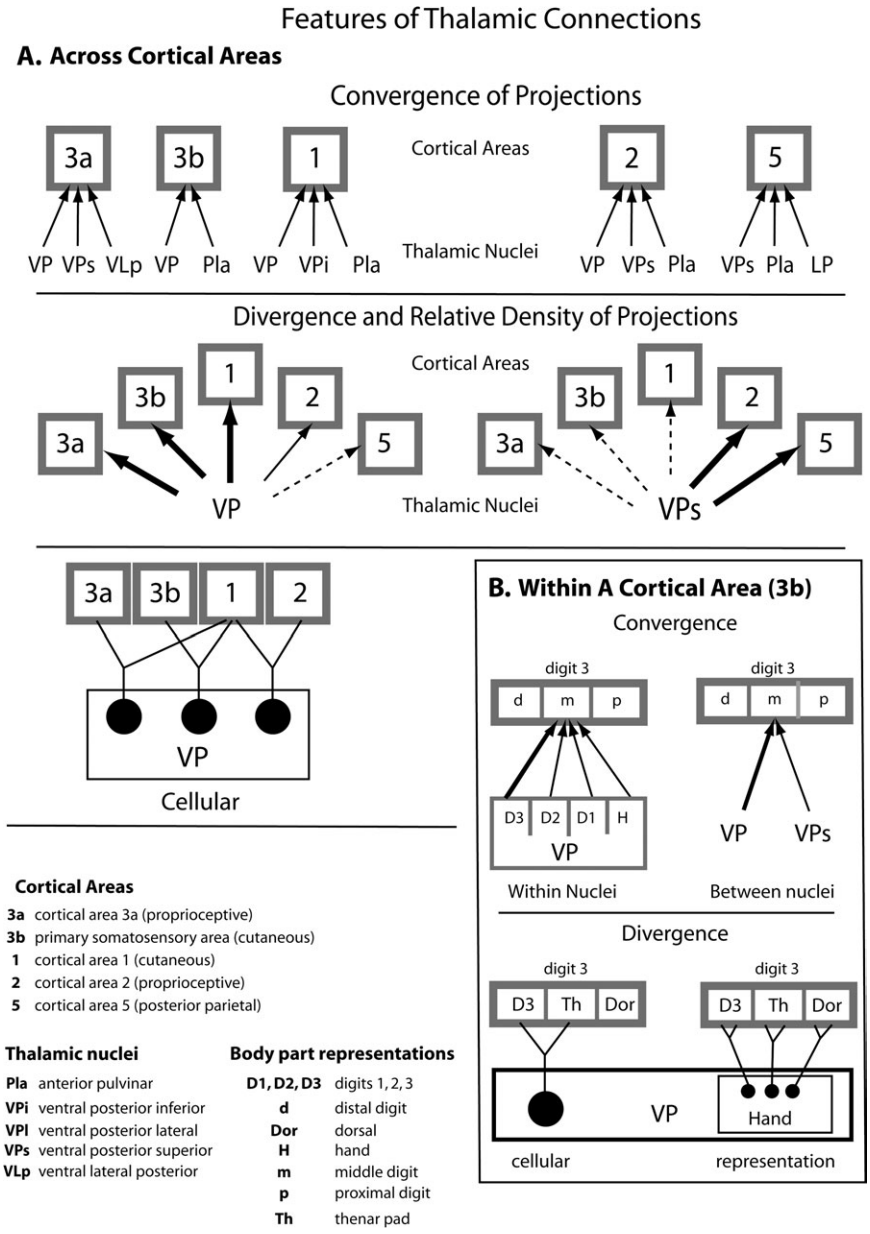

Figure 17. A summary of some of the major connection types observed between nuclei in the thalamus and cortical areas 3a, 3b, 1, 2, and 5. This summary is not meant to be exhaustive, but to illustrate the convergence and divergence in connections patterns across cortical areas (*A*), and within cortical areas (*B*). The top panel illustrates the high degree of convergence of thalamocortical projections observed for all cortical fields examined. A single cortical field gets inputs from at least 2 thalamic nuclei and sometimes as many as 5 thalamic nuclei. There is also a large amount of divergence observed in thalamocortical connectivity in that a given nucleus in the thalamus projects to multiple cortical areas. However, the density of projections differs for the different areas. For example, although VP projects to all cortical areas examined, its projections to area 3b and 1 are very dense, whereas those to area 5 are extremely sparse. Likewise, although VPs projects to all 5 areas investigated, the density of projections varied significantly. VPs had dense projections to areas 2 and 5 and relatively sparse connections to area 3a. This divergence was also observed at the cellular level (bottom left illustration). Thus, individual cells within a nucleus, such as VP projected to more than one field. Within a cortical area (*B*) convergence and divergence is observed for a given representation. For example, the representation of middle digit 3 in area 3b received convergent input from different body part representations within VP, such as from D3, D2, D1, and the hand, and also received convergent inputs from different nuclei in the thalamus. Further, divergence is observed at the cellular level and the level of the representation within a nucleus (*B*). Thus, the same neuron in VP can project to 2 different representations in 3b (D3 and the thenar pad), and the same representation in VP (hand) can project to different representations in 3b (D3, Th, Dor).

from studies of thalamocortical connections of individual cortical fields in a variety of primates, with an emphasis on studies in macaque monkeys. To our knowledge, there are no other studies in which up to 4 different anatomical tracers have been placed into the matched representations in 4 separate fields in the same animal so that the thalamocortical connectivity of these fields could be directly compared. We discuss each field individually for easier comparisons with previous studies, but conclude by considering the data from all anterior parietal fields.

Area 3b

There is a wealth of data in a variety of primates that demonstrates dense connections between the ventral posterior

nucleus and the primary somatosensory area of the cortex, area 3b (Jones and Powell 1970; Whitsel et al. 1978; Lin et al. 1979; Nelson and Kaas 1981; Jones et al. 1982; Cusick et al. 1985; Mayner and Kaas 1986; Cusick and Gould 1990; Darian-Smith et al. 1990; Krubitzer and Kaas 1992; Qi et al. 2002). One previous study examined the thalamocortical connections of 2 closely placed injections in area 3b (Rausell and Jones 1995) and found double-labeled cells in VP only when injections were less than 600 μm apart. In the present investigation, we observed double-labeled cells in VPl and VPs when injections were up to 2 mm apart. However, as in the previous study, most cells labeled from nearby injection sites in 3b in the present study resulted in labeled neurons in overlapping portions of VP (i.e., they were not double-labeled). Both the present and previous studies are consistent with results from experiments in macaque monkeys that directly examined the extent of arborization of thalamocortical axons in area 3b and found that the mean arborization was 600 μm, with the upper limit close to 3 mm (Garraghty and Sur 1990).

Only a few previous studies injected neuroanatomical tracers into electrophysiologically defined locations in VPl and recorded from locations in area 3b (e.g., Jones and Friedman 1982; Rausell et al. 1998). In the latter study 2 separate body part representations in VPl were injected with neuroanatomical tracers to examine the amount of convergence in thalamocortical projections to area 3b (although the locations in area 3b were not electrophysiologically defined). As in the present investigation, Rausell et al. (1998) observed a high degree of convergence in area 3b resulting from injections placed in separate locations in VPl. Likewise, single, relatively focal injections in VPm resulted in broadly distributed connections in area 3b, indicating a high degree of divergence. In the one case in which the injection site in VPm and the cortical projection zone in area 3b were electrophysiologically determined, an injection in the cheek pouch representation in VPm labeled terminals in the cheek pouch representation in area 3b as well as in cortex lateral to this location, in the expected representations of the face and oral structures (e.g., Cusick et al. 1986). The results of the present investigation are consistent with this previous study in that we demonstrate a high degree of convergence and divergence in thalamocortical connectivity between VPl and area 3b. However, we additionally demonstrate that somatotopically adjacent and functionally related representations in both VPl and VPs project to a single representation in 3b (convergence), and a restricted representation in VPl projects to multiple, functionally related sites in area 3b (divergence; Fig. 17*B*). Thus, an important contribution of the present study is a description of the precise pattern of connections from multiple body part representations within and across nuclei of the thalamus to functionally defined regions of the cortex.

The divergence of thalamic projections to multiple, functionally related sites in area 3b account for some of the somatotopic reorganization of this area that follows sensory loss or skilled learning. For example, previous studies in rodents (Cusick et al. 1986; Cusick et al. 1990) and primates (Jones 2000; Kaas 2000) demonstrate that nerve section and amputation result in rapid reorganization (within days to weeks) of cortical maps in area 3b (see Calford and Tweedale 1991 for reorganization over shorter time scales). Specifically, sectioning the median nerve (Merzenich, Kaas, Wall, Sur, et al. 1983) or amputation of a digit (Merzenich et al. 1984) were followed by expansions of the representations of the spared inputs into the denervated zone of cortex. Because the time course of recovery can be too rapid to be accounted for by sprouting of new connections, existing inputs to the cortex from representations of adjacent body parts or skin surfaces in nuclei in the thalamus could be unmasked and contribute to the reorganization process. Our results demonstrate that these somatotopically convergent inputs to the cortex exist, and could provide the substrate for much of the plasticity that occurs following peripheral sensory loss.

Changes in sensory experience can also cause alterations in somatotopic map organization (Recanzone, Jenkins, et al. 1992) which occurs over a period of days to months. As with sensory loss, convergent and divergent thalamic inputs may underlie the expansions of representations (Recanzone, Merzenich and Jenkins 1992), and may also mediate the temporal changes in neural processing that have been observed in area 3b with skilled use and learning (Recanzone, Merzenich, Jenkins, Grajski, et al. 1992; Recanzone, Merzenich and Schriener 1992).

Projections from VPs to area 3b were also observed in the present investigation, and these projections have been demonstrated in previous studies in macaque monkeys (e.g., Darian-Smith et al. 1990) as well as other primates (e.g., Cusick et al. 1986; Mayner and Kaas 1986; Krubitzer and Kaas 1992) although the terminologies sometimes differed (see above), or VPs appears to have been incorporated into the dorsal portion of VPl (e.g., Nelson and Kaas 1981). Although projections from other thalamic nuclei such as Pla, VLp and VPi to area 3b were observed in the present study as well as in previous studies, these projections were inconsistent and were variable between cases, species and studies. These inconsistencies may be due to different laminar termination patterns of different thalamic nuclei. Inputs from VPs to area 3b are particularly intriguing because this nucleus is relaying information from deep receptors of the muscles and joints to cutaneous representations of the cortex.

An interesting question is why the majority of the responses of neurons in area 3b are cutaneous in nature given this convergence of inputs from both cutaneous and deep nuclei of the thalamus to area 3b. This could be due to the selective activation of inputs from VP over those from VPs, which do not elicit action potentials in the postsynaptic neurons under normal conditions. An alternative explanation is that defining joint and muscle responses that underlie regions of skin with cutaneous responses is inherently problematic as the cutaneous response cannot be differentiated from the muscle or joint response using these techniques. The results from the current experiments predict that there should be at least subthreshold, if not suprathreshold responses to muscle and/or joint stimulation in area 3b neurons. Subthreshold convergent inputs from different topographic locations or submodalities that modulate and/or facilitate neural responses have been demonstrated in intracellular recording studies in area 3b of raccoons (Smits et al. 1991) and area 3a of cats (Kang et al. 1985). These functional studies, like the present anatomical study, provide strong evidence that such convergent inputs are in fact present, and likely contribute substantially to the reorganization that occurs following loss of sensory input, or skilled use.

Area 1

As with area 3b, thalamocortical connections of area 1 have been well studied in primates. In macaque monkeys (Nelson

and Kaas 1981; Darian-Smith et al. 1990), squirrel monkeys (Jones 1975; Cusick et al. 1986), owl monkeys (Lin et al. 1979), titi monkeys (Coq et al. 2004; Padberg and Krubitzer 2006), cebus monkeys (Mayner and Kaas 1986), and marmosets (Krubitzer and Kaas 1992) the ventral posterior nucleus has dense projections to area 1. We also observed moderate projections from VPs, Pla, and VPi (Fig. 7). Some previous studies in monkeys (Cusick et al. 1986) also observed projections from VPs, Pla, and VPi to area 1, whereas others (e.g., Nelson and Kaas 1981; Mayner and Kaas 1986) did not. However, the overall pattern of projections in previous studies in macaques is similar to the patterns observed in the present study, and it is possible that some nuclei, such as VPs, were actually incorporated into the boundaries of VPl. An interesting observation of the present study is that although identical portions of the hand representation in area 3b and 1 do receive inputs from the same neurons in VPl, the majority of projections are from different cells located in an overlapping region of VPl. This may be because projections from VP to area 1 are in layer 3, whereas projections from VP to area 3b terminate in layer 4 (Jones 1975), and thus different groups of neurons in VP project to different cortical layers. Further, it is possible that different classes of neurons in VP may be projecting differentially to the different layers in areas 3b and 1 (Kaas 2008).

Areas 3a and 2

Cortical areas 3a and 2 are distinct from areas 3b and 1 in terms of the submodality to which their neurons respond, and to a certain extent in their topographic organization (e.g., Krubitzer et al. 2004; Krubitzer and Disbrow 2008). Unlike 3b and 1, in which neurons respond to cutaneous stimulation, neurons in areas 3a and 2 respond to high threshold cutaneous stimulation, pressure, taps to the muscles, and joint and limb manipulation (Phillips et al. 1971; Schwarz et al. 1973; Heath et al. 1975; Hore et al. 1976; Pons et al. 1985; Huffman and Krubitzer 2001; Krubitzer et al. 2004; Padberg et al. 2007; Wang et al. 2007). Thus, both areas are involved in proprioception, and area 3a in particular has been shown to have interconnections with motor, premotor and posterior parietal areas of the neocortex (Jones et al. 1978; Huerta and Pons 1990; Darian-Smith et al. 1993; Huffman and Krubitzer 2001).

In the present study, the major sources of input to area 3a were from VLp, where neurons respond to stimulation of deep receptors, and VPl, where neurons respond to stimulation of cutaneous receptors. Other inputs were from VPs and VPi, but these were relatively sparse. Thus, area 3a has access to both deep and cutaneous inputs, and the latter inputs are in the same location of VPl as that projecting to area 3b (and sometimes even the same neurons). The inputs from VLp, VPs and VPi are not surprising given that neurons in area 3a respond to stimulation of muscles and joints. In microelectrode experiments in anesthetized monkeys the cutaneous inputs to area 3a are not always apparent, but when they are, they are often observed in the representation of the hand, as in the present study (e.g., Krubitzer et al. 2004). This convergence of connections from deep and cutaneous nuclei of the thalamus could account for the change in the submodality of the responses of neurons in area 3a following behavioral training (Jenkins et al. 1990; Recanzone, Merzenich, Jenkins, Grajski, et al. 1992). Specifically, there is a preponderance of responses to cutaneous stimulation in the region of area 3a that represents the stimulated or trained skin, rather than responses to muscle and joint stimulation.

There are several studies that have examined thalamocortical connections of area 3a in primates such as macaques (Friedman and Jones 1981; Darian-Smith et al. 1990), marmosets (Huffman and Krubitzer 2001) and squirrel monkeys (Akbarian et al. 1992). The results from these studies vary, although some of this variation is due to differences in the terminology used for what appear to be the same thalamic nuclei. For example, studies in macaque monkeys (e.g., Jones et al. 1979; Friedman and Jones 1981; Darian-Smith et al. 1990) report that area 3a receives input from the deep shell region of VPl (c), which coincides with what we term VPs, from VPl proper (Jones and Friedman 1982; Darian-Smith et al. 1990), and VPLo (our VLp). Studies in New World monkeys such as marmosets and squirrel monkeys reveal a similar pattern of connectivity as that described in the present investigation in that area 3a receives inputs from VL, VP proper, VPs (Akbarian et al. 1992; Huffman and Krubitzer 2001), and Pla (not observed in the present study.

There are only 2 studies that have injected anatomical tracers into electrophysiologically defined locations in area 2 and examined the total pattern of thalamocortical connections in primates, these include the study by Pons and Kaas (1985b) in macaque monkeys, and a recent study in the New World cebus monkey (Franca et al. 2008). In both the current study and previous studies in macaques, area 2 receives its inputs from VPs the Pla and VPl. We also observed sparse inputs from VLp, LP, and VPi. Results in cebus monkeys are interesting given that connections of area 2 in this species appear to have evolved independently from those in macaques (Padberg et al. 2007). As in macaques, the major sources of input to area 2 are from Pla and VPs with moderate inputs from VPl and VPi. Area 2 in cebus monkeys also receives inputs from VA and VLp. Thus, area 2 in both species receives inputs from nuclei relaying information from deep receptors (VPs and VLp) as well as cutaneous receptors (VPl and Pla), consistent with the submodalities to which neurons in area 2 respond. As with other anterior parietal fields, most neurons that project to area 2 from VPl are in locations that project to anterior parietal areas 3a, 3b and 1, and some of the same neurons project to area 2 and other fields, such as area 3b or area 1.

Projections of Single Neurons to more than One Cortical Field

In the present study we found small numbers of neurons that were labeled by separate injections in different somatosensory areas (Fig. 7*G*). The majority of these double-labeled cells were observed in the VP, with fewer double-labeled cells observed in VPs and VLp. Previous results have been used to argue for or against thalamic neurons projecting to more than one area (e.g., Jones 1983; Darian-Smith et al. 1993; see Cusick et al. 1985, for review). It is difficult to relate the results of some of these previous studies with our own findings because in previous studies injection sites were not matched for somatotopic location, and/or injection sites may have spread into each other and contaminated the results. In our opinion, the study of Cusick et al. (1985) is most compelling because separate injections in the digit tip representations along the 3b/3a border and along the 3b/1 border in squirrel monkeys, where these areas are on the brain surface, clearly

double-labeled substantial numbers of neurons in VP, VPs, and Pla. Although fewer double-labeled cells were found in the present study, this could reflect species differences as well as differences in the size of injections and the amount of somatotopic overlap of maps in these fields.

Thalamocortical Connections of Area 5

Traditionally area 5 is considered to be a higher order area positioned at the end of a hierarchy in which information is serially processed in anterior parietal cortex (areas 3b to area 1 to area 2) before it is fed forward and processed in area 5. Support for this idea comes from electrophysiological recording studies in area 5 in macaque monkeys which demonstrate that neurons have more complex receptive fields that can be modulated by attention states and modified by experience (e.g., Mountcastle et al. 1975; Iwamura et al. 1994; Iriki et al. 1996a, 1996b; Graziano et al. 2000; Iwamura et al. 2002; see Krubitzer and Disbrow 2008, for review; also see Hsiao et al. 1993; Burton and Sinclair 2000; Steinmetz et al. 2000; Meftah et al. 2002, for attention effects in other areas). Further, unlike anterior parietal fields which are proposed to be involved in more simple discriminations of object texture, shape and size (e.g., Randolph and Semmes 1974; Carlson 1981), area 5 is thought to be a region that generates an internal coordinate system for intentional reaching and grasping into immediate extra personal space (e.g., Ferraina and Bianchi 1994; Lacquaniti et al. 1995; Snyder et al. 1997; see Wise et al. 1997; Debowy et al. 2001; Krubitzer and Disbrow 2008, for review). In the present investigation we observed that area 5 received sparse projections from VP, VPi, and VLp and dense projections from VPs, Pla, and LP. VPs processes inputs from muscles and joints, and such inputs would be necessary for generating an internal representation of the body. Interestingly area 5 also receives input from VPl and Pla, which process cutaneous inputs.

There is only one other study in macaque monkeys in which thalamocortical connections were examined by placing neuroanatomical tracers into the electrophysiologically identified hand representation in area 5 (Pons and Kaas 1985b). In this study connections were observed with Pla, VPs, and ventral LP. Further, sparse projections were observed from VPl. There were several previous studies in macaque monkeys where tracers were injected relative to sulcal patterns (e.g., Jones et al. 1979; Yeterian and Pandya 1985; Schmahmann and Pandya 1990). Resulting patterns of label in the thalamus in these studies was similar but not identical to the patterns of connections observed in the present investigation. In New World cebus monkeys (Franca et al. 2008) the major inputs to electrophysiologically identified locations in area 5 were from VL, Pla, and VPl, whereas in titi monkeys the major inputs were from VL and Pla with moderate inputs from a number of other nuclei including VPl, CL, and VPs (Padberg and Krubitzer 2006). Thus, the overall pattern of thalamocortical connectivity of area 5 appears to be somewhat different in New World versus Old World monkeys, and in titi monkeys connections are more broadly distributed than in cebus and macaque monkeys. These neuroanatomical differences could be due, in part, to the different structure of the hand and use of the hand in New World monkeys (except the cebus) compared with Old World monkeys, and may underlie the differences in manual dexterity and grasping abilities that each group displays.

Specializations of Somatosensory Processing

One issue that should be kept in mind is that the injections in the present study (and most previous studies) were all made in the hand representation in the different cortical regions. This was done for 2 reasons. First, macaque monkeys are very tactile animals and primarily use their hands to manipulate their environment. Thus, akin to studying the barrel cortex in rodents, the hand representation in macaques is a highly specialized cortical structure. Second, it is least difficult to make injections in similar body part representations between cortical areas and different body part representations within a cortical area if one targets the hand representation. This allows, for the first time, a comprehensive study in individual animals while limiting the spread of the injections across body part and/or cortical boundaries. This raises the issue of whether the hand representation is more specialized in its thalamocortical connections compared with other body part representations.

There is both functional and anatomical evidence that indicates that the hand representation in anterior and posterior parietal cortex in primates is specialized. For example, as noted in the Introduction (Fig. 1), there is a large magnification of the representation of the hand in somatosensory cortex, and this is especially pronounced in posterior parietal area 5. Studies of cortical connections of the hand/forelimb versus other body part representations also demonstrate differences. For example, in marmosets, injections in the forelimb representation in area 3a resulted in more broadly distributed connections with posterior parietal cortex than injections in the hindlimb representation (Huffman and Krubitzer 2001), and in area 5 in titi monkeys, the digit tip representation has a greater density of connections with motor cortex, premotor cortex and with areas 7b/AIP than does the hairy hand representation (Padberg et al. 2005). Differences were also noted in thalamocortical connections of these studies in that the forelimb and hand representations in area 3a received denser projections from VPs, MD, and CL compared with the hindlimb representation (Huffman and Krubitzer 2001). In titi monkeys, the digit tips representation in area 5 received greater input from VL, CL, and MD than did the representation of the hairy hand (Padberg and Krubitzer 2006). Although the possibility that thalamocortical connections of anterior and posterior parietal cortex in primates is specialized compared to other body part representations has some experimental support, more detailed, systematic studies need to be carried out to further define these specializations.

The somatosensory system in general appears to have several unique features of processing that are not observed in other sensory systems. For example, there is a very close association of somatosensory areas of the cortex with motor nuclei of the thalamus, in that VLp projects not only to area 3a, but also projects sparsely to areas 3b, 1, 2, and 5. This interaction between the somatosensory and motor system is even more pronounced at the level of the cortex where all anterior parietal fields and posterior parietal area 5 have interconnections with motor cortex, premotor cortex or both (see Krubitzer and Disbrow 2008, for review). Finally, the high degree of convergent input from functionally related body part representations in the thalamus to a single representation in the cortex is also a distinguishing feature of this system. These differences may be due to the distinct way in which the

somatosensory system is used compared with the visual and auditory systems. Unlike other sensory systems, the body dynamically interacts with the object to be explored and this interaction is critical for identifying features of the object such as size, weight, texture and composition. This process requires continual updating from tactile and proprioceptive inputs across functionally related parts of the hand regarding the current position of the digits, hand, wrist and forelimb. Such integrated information processing is necessary for reaching, grasping and manipulating objects in extra personal space, and for generating an appropriate internal coordinate system necessary for these manual behaviors.

Funding

NINDS grant (R01-NS35103) to L.K.; NEI grant (R01-EY013458) to G.R.; and NIH grant (R01-NS16446) to J.K.

Notes

We wish to thank Rebecca Grunewald for help with histological preparation of tissue and data reconstruction. *Conflict of Interest*: None declared.

Address correspondence to Leah Krubitzer, PhD, Center for Neuroscience, 1544 Newton Ct, Davis, CA 95618, USA. Email: lakrubitzer@ucdavis.edu.

References

Akbarian S, Grusser OJ, Guldin WO. 1992. Thalamic connections of the vestibular cortical fields in the squirrel monkeys (*Saimiri sciureus*). J Comp Neurol. 326:423–441.

Bruce K, Grofova I. 1992. Notes on a light and electron microscopic double-labeling method combining anterograde tracing with phaseolus vulgaris leucoagglutinin and retrograde tracing with cholera toxin subunit b. J Neurosci Methods. 45:23–33.

Burton H, Sinclair RJ. 2000. Tactile-spatial and cross-modal attention effects in the primary somatosensory cortical areas 3b and 1-2 of rhesus monkeys. Somatosens Mot Res. 17:213–228.

Calford MB, Tweedale R. 1991. Immediate expansion of receptive fields of neurons in area 3b of macaque monkeys after digit denervation. Somatosens Mot Res. 8:249–260.

Carlson M. 1981. Characteristics of sensory deficits following lesions of Brodmann's areas 1 and 2 in the postcentral gyrus of *Macaca mulatta*. Brain Res. 204:424–430.

Celio MR. 1990. Calbindin D-28k and parvalbumin in the rat nervous system. Neuroscience. 35:375–475.

Coq JO, Qi HX, Collins CE, Kaas JH. 2004. Anatomical and functional organization of somatosensory areas of the lateral fissure in the new world titi monkeys (*Callicebus moloch*). J Comp Neurol. 476: 363–387.

Craig AD. 2008. Retrograde analyses of spinothalamic projections in the macaque monkey: input to the ventral lateral nucleus. J Comp Neurol. 508:315–328.

Craig AD, Zhang ET. 2006. Retrograde analyses of spinothalamic projections in the macaque monkey: input to posterolateral thalamus. J Comp Neurol. 499:953–964.

Cusick CG, Gould HJ, 3rd. 1990. Connections between area 3b of the somatosenosry cortex and subdivisions of the ventralposterior nuclear complex and the anterior pulvinar nucleus in squirrel monkeys. J Comp Neurol. 292:83–102.

Cusick CG, Steindler DA, Kaas JH. 1985. Corticocortical and collateral thalamocortical connections of postcentral somatosensory cortical areas in squirrel monkeys: a double-labeling study with radiolabeled wheatgerm agglutinin and wheatgerm agglutinin conjugated to horseradish peroxidase. Somatosens Mot Res. 3:1–31.

Cusick CG, Wall JT, Kaas JH. 1986. Representations of the face, teeth, and oral cavity in areas 3b and 1 of somatosensory cortex in squirrel monkeys. Brain Res. 370:359–364.

Cusick CG, Wall JT, Whiting JJ, Wiley RG. 1990. Temporal progression of cortical reorganization following nerve injury. Brain Res. 537:355–358.

Darian-Smith C, Darian-Smith I, Burman K, Ratcliffe N. 1993. Ipsilateral cortical projections to areas 3a, 3b, and 4 in the macaque monkey. J Comp Neurol. 335:200–213.

Darian-Smith C, Darian-Smith I, Cheema SS. 1990. Thalamic projections to sensorimotor cortex in the macaque monkey: Use of multiple retrograde fluorescent tracers. J Comp Neurol. 299:17–46.

Debowy DJ, Ghosh S, Ro JY, Gardner EP. 2001. Comparison on neuronal firing rates in somatosensory and posterior parietal cortex during prehension. Exp Brain Res. 137:269–291.

Disbrow EA, Huffman KJ, Recanzone G, Krubitzer LA. 2000. The connections of areas 5 and 2 with electrophysiologically identified somatosensory cortical areas in macaque monkeys. Soc Neurosci Abstr. 26:2082.

Disbrow E, Litinas E, Recanzone G, Padberg J, Krubitzer LA. 2003. Cortical connections of the parietal ventral area and the second somatosensory area in macaque monkeys. J Comp Neurol. 462:382–399.

Disbrow E, Litinas E, Recanzone G, Slutsky D, Krubitzer LA. 2002. Thalamocortical connections of the parietal ventral area (pv) and the second somatosensory area (s2) in macaque monkeys. Thalamus Relat Syst. 1:289–302.

Dykes RW, Sur M, Merzenich MM, Kaas JH, Nelson RJ. 1981. Regional segregation of neurons responding to quickly adapting, slowly adapting, deep and pacinian receptors within thalamic ventroposterior nuclei in the squirrel monkey (Saimiri sciureus). Neuroscience. 6:1687–1692.

Evrard HC, Craig AD. 2008. Retrograde analysis of the cerebellar projections to the posteroventral part of the ventral lateral thalamic nucleus in the macaque monkey. J Comp Neurol. 508:286–314.

Fang PC, Stepniewska I, Kaas JH. 2006. The thalamic connections of motor, premotor, and prefrontal areas of cortex in a prosimian primate (Otolemur garnetti). Neuroscience. 143:987–1020.

Ferraina S, Bianchi L. 1994. Posterior parietal cortex: functional properties of neurons in area 5 during an instructed-delay reaching task within different parts of space. Exp Brain Res. 99:175–178.

Franca JG, Padberg J, Bittencourt-Navarrete RE, Soares JG, Amanicio GJO, Cooke DR, Rajan AT, Fiorani M, Gattass R, Krubitzer L. 2008. Thalamocortical connections of areas 1, 2 and 5 in the New World cebus monkey (Cebus apella). 38th annual meeting of the Society for Neuroscience; Nov 15-19; Washington, DC. Washington, DC: Society for Neuroscience. Program No. 370.1.

Friedman D, Jones E. 1981. Thalamic input to areas 3a and 2 in monkeys. J Neurophysiol. 45:59–85.

Friedman DP, Murray EA. 1986. Thalamic connectivity of the second somatosensory area and neighbouring somatosensory fields of the lateral sulcus of the macaque. J Comp Neurol. 252:348–373.

Gardner E. 1988. Somatosensory cortical mechanisms of feature detection in tactile and kinesthetic discrimination. Can J Physiol Pharmacol. 66:439–454.

Garraghty PE, Sur M. 1990. Morphology of single intracellularly stained axons terminating in area 3b of macaque monkeys. J Comp Neurol. 294:583–593.

Graziano MSA, Cooke DF, Taylor CSR. 2000. Coding the location of the arm by sight. Science. 290:1782–1786.

Heath CJ, Hore J, Philips CG. 1975. Inputs from low threshold muscle and cutaneous afferents of hand and forearm to areas 3a and 3b of baboon's cerebral cortex. J Physiol (Lond). 257:199–227.

Hendry SHC, Jones EG, Hockfield S, McKay RDG. 1988. Neuronal populations stained with the monoclonal antibody Cat-301 in the mammalian cerebral cortex and thalamus. J Neurosci. 8:518–542.

Hockfield S, McKay RD, Hendry SHC, Jones EG. 1983. A surface antigen that identifies ocular dominance columns in the visual cortex and laminar features of the lateral geniculate nucleus. Cold Spring Harbor Symp Quant Biol. 48:877–889.

Hore J, Preston JB, Cheney PD. 1976. Responses of cortical neurons (areas 3a and 4) to ramp stretch of hindlimb muscles in the baboon. J Neurophysiol. 39:484–500.

Hsiao SS, O'Shaughnessy DM, Johnsson KO. 1993. Effects of selective attention on spatial form processing in monkey primary and secondary somatosensory cortex. J Neurophysiol. 70:444–447.

Huerta MF, Pons TP. 1990. Primary motor cortex receives input from area 3a in macaques. Brain Res. 537:367–371.
Huffman KJ, Krubitzer L. 2001. Area 3a: Topographic organization and cortical connections in marmoset monkeys. Cereb Cortex. 11:849–867.
Iriki A, Tanaka M, Iwamura Y. 1996a. Attention-induced neuronal activity in monkey somatosensory cortex revealed by pupillometrics. Neurosci Res. 25:173–181.
Iriki A, Tanaka M, Iwamura Y. 1996b. Coding of modified body schema during tool use by macaque postcentral neurons. NeuroReport. 7:2325–2330.
Iwamura Y, Iriki A, Tanaka M. 1994. Bilateral hand representation in the postcentral somatosensory cortex. Nature. 369:554–556.
Iwamura Y, Tanaka M, Iriki A, Taoka M, Toda T. 2002. Processing of tactile and kinesthetic signals from bilateral sides of the body in the postcentral gyrus of awake monkeys. Behav Brain Res. 135:185–190.
Jenkins WM, Merzenich MM, Ochs MT, Allard T, Guíc Robles E. 1990. Functional reorganization of primary somatosensory cortex in adult owl monkeys after behaviorally controlled tactile stimulation. J Neurophysiol. 63:82–104.
Jones EG. 1975. Lamination and differential distribution of thalamic afferents within the sensory-motor complex of the squirrel monkey. J Comp Neurol. 160:167–203.
Jones EG. 1983. Lack of collateral thalamocortical projections to fields of the first somatic sensory cortex in monkeys. Exp Brain Res. 52:375–384.
Jones EG. 2000. Cortical and subcortical contributions to activity-dependent plasticity in primate somatosensory cortex. Annu Rev Neurosci. 23:1–37.
Jones EG. 2007. The thalamus. Cambridge: University Press.
Jones EG, Coulter JD, Hendry SHC. 1978. Intracortical connectivity of architectonic fields in the somatic sensory, motor and parietal cortex of monkeys. J Comp Neurol. 181:291–348.
Jones EG, Friedman DP. 1982. Projection pattern of functional components of thalamic ventrobasal complex on monkey somatosensory cortex. J Neurophysiol. 48:521–544.
Jones EG, Friedman DP, Hendry SC. 1982. Thalamic basis of place- and modality-specific columns in monkey somatosensory cortex: a correlative anatomical and physiological study. J Neurophysiol. 48:545–568.
Jones EG, Powell TPS. 1970. Connexions of the somatic sensory cortex of the rhesus monkey iii. Thalamic connexions. Brain. 93:37–56.
Jones EG, Wise SP, Coulter JC. 1979. Differential thalamic relationships of sensory-motor and parietal cortical fields in monkeys. J Comp Neurol. 183:833–882.
Kaas JH. 2000. The reorganization of somatosensory and motor cortex after peripheral nerve or spinal cord injury in primates. Prog Brain Res. 128:173–179.
Kaas JH. 2008. The somatosensory thalamus and associated pathways. In: Gardner E, Kaas JH, editors. Somatosensation. London: Elsevier. p. 117–141.
Kaas JH, Nelson RJ, Sur M, Dykes RW, Merzenich MM. 1984. The somatotopic organization of the ventroposterior thalamus of the squirrel monkey, *Saimiri sciureus*. J Comp Neurol. 226:111–140.
Kang R, Herman D, MacGillis M, Zarzecki P. 1985. Convergence of sensory inputs in somatosensory cortex: interactions from separate afferent sources. Exp Brain Res. 57:271–278.
Krubitzer L, Clarey J, Tweedale R, Calford M. 1998. Interhemispheric connections of somatosensory cortex in the flying fox. J Comp Neurol. 402:538–559.
Krubitzer L, Disbrow E. 2008. The evolution of parietal areas involved in hand use in primates. In: Gardner E, Kaas JH, editors. Somatosensation. London: Elsevier. p. 183–214.
Krubitzer LA, Huffman KJ, Disbrow E, Recanzone GH. 2004. Organization of area 3a in macaque monkeys: contributions to the cortical phenotype. J Comp Neurol. 471:97–111.
Krubitzer LA, Kaas JH. 1992. The somatosensory thalamus of monkeys: Cortical connections and a redefinition of nuclei in marmosets. J Comp Neurol. 319:123–140.
Lacquaniti F, Guigon E, Bianchi L, Ferraina S, Caminiti R. 1995. Representing spatial information for limb movement: the role of area 5 in monkey. Cereb Cortex. 5:391–409.
Lin CS, Merzenich MM, Sur M, Kaas JH. 1979. Connections of areas 3b and 1 of the parietal somatosensory strip with the ventroposterior nucleus in the owl monkey, *Aotus trivirgatus*. J Comp Neurol. 185:355–372.
Loe PR, Whitsel BL, Dreyer DA, Metz CB. 1977. Body representation in ventrobasal thalamus of macaque: a single-unit analysis. J Neurophysiol. 40:1339–1355.
Macchi G, Jones EG. 1997. Toward an agreement on terminology of nuclear and subnuclear divisions of the motor thalamus. J Neurosurg. 86:670–685.
Mayner L, Kaas J. 1986. Thalamic projections from electrophysiologically defined sites of body surface representations in areas 3b and 1 of somatosensory cortex of cebus monkeys. Somatosens Res. 4:13–29.
Meftah el-M, Shenasa J, Chapman CE. 2002. Effects of a cross-modal manipulation of attention on somatosensory cortical neuronal responses to tactile stimuli in the monkey. J Neurophysiol. 88:3133–3149.
Merzenich MM, Kaas JH, Wall J, Nelson RJ, Sur M, Felleman D. 1983. Topographic reorganization of somatosensory cortical areas 3b and 1 in adult monkeys following restricted deafferentation. Neuroscience. 8:33–55.
Merzenich MM, Kaas JH, Wall JT, Sur M, Nelson RJ, Felleman DJ. 1983. Progression of change following median nerve section in the cortical representation of the hand in areas 3b and 1 in adult owl and squirrel monkeys. Neuroscience. 10:639–665.
Merzenich MM, Nelson RJ, Stryker MP, Cynader MS, Schoppmann A, Zook JM. 1984. Somatosensory cortical map changes following digit amputation in adult monkeys. J Comp Neurol. 224:591–605.
Mountcastle VB, Henneman E. 1952. The representation of tactile sensibility in the thalamus of the monkey. J Comp Neurol. 97:409–489.
Mountcastle VB, Lynch JC, Georgopoulos A, Sakata H, Acuña C. 1975. Posterior parietal association cortex of the monkey: command functions for operations within extrapersonal space. J Neurophysiol. 38:871–908.
Nelson RJ, Kaas JH. 1981. Connections of the ventroposterior nucleus of the thalamus with the body surface representations in cortical areas 3b and 1 of the cynomologus macaque, *Macaca fascicularis*. J Comp Neurol. 199:29–64.
Nelson RJ, Sur M, Felleman DJ, Kaas JH. 1980. Representations of the body surface in postcentral parietal cortex of Macaca fascicularis. J Comp Neurol. 192:611–643.
Padberg J, Disbrow E, Krubitzer L. 2005. The organization and connections of anterior and posterior parietal cortex in titi monkeys: do new world monkeys have an area 2? Cereb Cortex. 15:1938–1963.
Padberg J, Franca JG, Cooke DF, Soares JG, Rosa MG, Fiorani M, Gattass R, Krubitzer L. 2007. Parallel evolution of cortical areas involved in skilled hand use. J Neurosci. 27:10106–10115.
Padberg J, Krubitzer LA. 2006. Thalamocortical connections of anterior and posterior parietal cortex in titi monkeys. J Comp Neurol. 497:416–435.
Phillips CB, Powell TPS, Wiesandanger M. 1971. Projections from low threshold muscle afferents of hand and forearm to area 3a of baboon's cortex. J Physiol. 217:419–446.
Poggio GF, Mountcastle VB. 1963. The functional properties of ventrobasal thalamic neurons studied in unanesthetized monkeys. J Neurophysiol. 26:775–806.
Pons TP, Garraghty PE, Cusick CG, Kaas JH. 1985. The somatotopic organization of area 2 in macaque monkeys. J Comp Neurol. 241:445–466.
Pons TP, Kaas JH. 1985. Connections of area 2 of somatosensory cortex with the anterior pulvinar and subdivisions of the ventroposterior complex in macaque monkeys. J Comp Neurol. 240:16–36.

Qi HX, Lyon DC, Kaas JH. 2002. Cortical and thalamic connections of the parietal ventral somatosensory area in marmoset monkeys (Callithrix jacchus). J Comp Neurol. 443:168–182.
Randolph M, Semmes J. 1974. Behavioral consequences of selective subtotal ablations in the postcentral gyrus of *Macaca mulatta*. Brain Res. 70:55–70.
Rausell E, Bickford L, Manger PR, Woods TM, Jones EG. 1998. Extensive divergence and convergence in the thalamocortical projection to monkey somatosensory cortex. J Neurosci. 18:4216–4231.
Rausell E, Jones EG. 1991. Histochemical and immunocytochemical compartments of the thalamic vpm nucleus ain monkeys and their relationship to the representational map. J Neurosci. 11:210–225.
Rausell E, Jones EG. 1995. Extent of intracortical arborization of thalamocortical aoxns as a determinant of representational plasticity in monkey somatic sensory cortex. J Neurosci. 15:4270–4288.
Recanzone GH, Jenkins WM, Hradek GT, Merzenich MM. 1992. Progressive improvement in discriminative abilities in adult owl monkeys performing a tactile frequency discrimination task. J Neurophysiol. 67:1015–1030.
Recanzone GH, Merzenich MM, Jenkins WM. 1992. Frequency discrimination training engaging a restricted skin surface results in an emergence of a cutaneous response zone in cortical area 3a. J Neurophysiol. 67:1057–1070.
Recanzone GH, Merzenich MM, Jenkins WM, Grajski KA, Dinse HR. 1992. Topographic reorganization of the hand representation in cortical area 3b of owl monkeys trained in a frequency discrimination task. J Neurophysiol. 67:1031–1056.
Recanzone GH, Merzenich MM, Schriener CE. 1992. Changes in the distributed temporal response properties of si cortical neurons reflect improvements in performance on a temporally based tactile discrimination task. J Neurophysiol. 67:1057–1070.
Schmahmann JD, Pandya DN. 1990. Anatomical investigation of projections from thalamus to posterior parietal cortex in the rhesus monkey: a wga-hrp and fluorescent tracer study. J Comp Neurol. 295:299–326.
Schwartz A. 1983. Functional relationship between somatosensory cortex and specialized afferent pathways in the monkey. Exp Neurol. 79:316–328.
Schwarz DW, Deeck L, Fredrickson JM. 1973. Cortical projections of group i muscle afferents to areas 2, 3a, and the vestibular field in the rhesus monkey. Exp Brain Res. 17:516–526.
Sherman SM, Guillery RW. 2006. Exploring the thalamus and its role in cortical function. Cambridge: MIT Press.
Smits E, Gordon DC, Witte S, Rasmusson DD, Zarzecki P. 1991. Synaptic potentials evoked by convergent somatosensory and corticocortical inputs in raccoon somatosensory cortex: substrates for plasticity. J Neurophysiol. 66:688–695.
Snyder LH, Batista AP, Andersen RA. 1997. Coding of intention in the posterior parietal cortex. Nature. 386:167–170.
Steinmetz PN, Roy A, Fitzgerald PJ, Hsiao SS, Johnson KO, Niebur E. 2000. Attention modulates synchronized neuronal firing in primate somatosensory cortex. Nature. 404:187–190.
Stepniewska I, Sakai ST, Qi HX, Kaas JH. 2003. Somatosensory input to the ventrolateral thalamic region in the macaque monkey: potential substrate for parkinsonian tremor. J Comp Neurol. 455:378–395.
Wang X, Zhang M, Cohen IS, Goldberg ME. 2007. The proprioceptiver-epresentation of eye position in monkey primary somatosensory cortex. Nat Neurosci. 10:640–646.
Whitsel BL, Rustioni A, Dreyer DA, Loe PR, Allen EE, Metz CB. 1978. Thalamic projections to s-i in macaque monkey. J Comp Neurol. 178:385–410.
Wiesendanger M, Miles TS. 1982. Ascending pathway of low-threshold muscle afferents to the cerebral cortex and its possible role in motor control. Physiol Rev. 62:1234–1270.
Wise SP, Boussaoud D, Johnson PB, Caminiti R. 1997. Premotor and parietal cortex: corticocortical connectivity and combinatorial computations. Annu Rev Neurosci. 20:25–42.
Wong-Riley M. 1979. Changes in the visual system of monocularly sutured or enucleated cats demonstrable with cytochrome oxidase histochemistry. Brain Res. 171:11–28.
Yeterian EH, Pandya DN. 1985. Corticothalamic connections of the posterior parietal cortex in the rhesus monkey. J Comp Neurol. 237:408–426.